

Node-wise monotone barrier coupling law for central pattern generation*

Jin Gyu Lee^{a,*}, Cyrus Mostajeran^b, Graham Van Goffrier^c

^aASRI, Department of Electrical and Computer Engineering, Seoul National University, Seoul, South Korea

^bDepartment of Engineering, University of Cambridge, Cambridge, United Kingdom

^cDepartment of Physics and Astronomy, University College London, London, United Kingdom

Abstract

With the aim of providing new insights into the mechanisms behind the emergence of collective behaviors via nonlinear coupling, we propose a node-wise monotone barrier coupling law that imitates the behavior and beneficial properties of neural central pattern generators (CPGs). In particular, the coupling law 1) allows us to assign multiple central patterns on the circle and 2) allows for rapid switching between different patterns via simple ‘kicks’. In the end, we achieve full control by partitioning the state space by utilizing a barrier effect and assigning unique steady-state behaviors to each element of the resulting partition. We analyze the global behavior and study the viability of the design.

Keywords: Neural central pattern generators, formation control, nonlinear spaces, positivity, consensus

1. Introduction

Phenomena where multiple agents synchronize in some sense to result in the emergence of collective behaviors are frequently observed in nature, complex ecosystems, social networks, financial markets, and energy networks. It is expected that a detailed understanding of the various mechanisms behind such phenomena will provide new modes of acquiring, processing, disseminating, and reacting to information and data.

Indeed, studies of synchronous oscillations in linearly coupled non-identical nonlinear oscillators observed in power grids and biological systems [1, 2, 3, 4] have provided us with a general theory on the collective behavior of a heterogeneous network under linear coupling [5, 6]. The network design tool further developed by this general theory has provided control techniques relevant for the design of smart and resilient societies. Examples include the use of distributed optimization to solve economic dispatch problems, i.e. to minimize the total generation cost under the power supply-demand balance and individual generation capacity constraints [7], distributed state estimation for the design of sensor networks where each sensor node can autonomously collect, manage, and control the information [8, 9], and the distributed SLAM problem where the goal is to make a group of mobile robots simultaneously localize and map the environment [10].

Meanwhile, more general types of coupling, i.e. nonlinear and/or non-smooth couplings, and more general state spaces, e.g. nonlinear spaces such as Lie groups [11,

12, 13, 14], the n -sphere [15], Grassmannians [16], and Stiefel manifolds [17], frequently appear in the modeling of physical, biological, or societal systems. Understanding the mechanism behind the enforcement of synchronization for heterogeneous agents and the emergence of collective behavior under this more general setting will provide additional beneficial features that are completely absent in linear models.

A particularly important example where we can see such features is that of the neural central pattern generators (CPGs) that produce diverse rhythms in networks for the purpose of collectively generating movements such as breathing, chewing, swallowing, walking, and heart beating [18] in animals. Understanding the mechanisms behind the control and regulation of CPGs may result in technological advances resulting in systems that can accommodate rapidly to sudden changes similar to the way that CPGs adapt in fractions of a second to respond to events, e.g. in choking prevention or predator escape [18]. Besides the ability to accommodate multiple central patterns in the network and rapidly switch between them, such systems also exhibit robustness with respect to individual variability. Indeed, in the study of a network of non-identical neurons interconnected via excitatory synaptic coupling, it was shown that the network is robust to heterogeneity and has the emergent behavior of synchronous spiking, even with the weak coupling strength and the impulsive nature of communication [19, 20]. This network is a particular case of the general representation of the CPGs by its absence of inhibitory synaptic coupling, which has the central pattern of synchronous spiking.

However, the theory for understanding such systems is only in its infancy. For instance, the mechanisms of CPGs have been extensively investigated in robotics to build autonomous robots that adapt efficiently to changing environments, but a solid theoretical understanding of the robust and adaptive hardware of CPGs is still lacking [21] and [20] is the only theoretical work that we are aware of on a network of heterogeneous neurons (using a conductance-based model) after nearly 30 years since the pioneering

*J.G.L. was supported by the National Research Foundation of Korea grant funded by the Korea government (Ministry of Science and ICT) under No. NRF-2017R1E1A1A03070342. C.M. was supported by a Henslow Research Fellowship from the Cambridge Philosophical Society. G.V.G. was supported by the UCL Centre for Doctoral Training in Data Intensive Science funded by STFC, and by an Overseas Research Scholarship from UCL.

*Corresponding author

Email addresses: jingyulee.scholar@gmail.com (Jin Gyu Lee), cyrus.mostajeran@gmail.com (Cyrus Mostajeran), graham.vangoffrier.19@ucl.ac.uk (Graham Van Goffrier)

work of Somers and Kopell on a network of identical neurons [22]. This lack of understanding particularly applies to synchronization enforceability and associated emergent collective behavior. In particular, consensusability, a prerequisite for synchronization enforceability, which answers the question of when does a network achieve consensus when there are no individual dynamics, has been studied for decades and only recently been understood under more general types of coupling [23].

Thus, to gain a deeper insight into such systems, in this paper we focus on the problem of formation control on the circle and propose a node-wise monotone barrier coupling law, motivated by our previous work on edge-wise coupling law [24], that is capable of exhibiting some of the attractive properties of CPGs. In particular,

1. it allows us to assign multiple central patterns in the steady-state behavior of the network with possibly different formations and common angular frequencies,
2. it allows rapid switching between different central patterns via a ‘simple kick’ or sudden disturbance,

and it brings robustness with respect to individual variability. For the proposed node-wise coupling law, we concentrate on the question of the viability of assigning one or several central patterns in the network, from an engineering viewpoint.

Consensus problems on nonlinear spaces give rise to behaviors and global convergence issues that are not observed in linear models [25]. Geometric consensus algorithms can be formulated intrinsically on a Riemannian manifold or extrinsically when the manifold is embedded in a Euclidean space. Most intrinsic consensus algorithms are based on the concepts of Riemannian distances, gradients, geodesics, and means. A fundamental challenge presented by consensus in nonlinear spaces is due to the non-uniqueness of geodesics and topological properties of the underlying space, which result in problems that are fundamentally more complex and interesting than Euclidean analogues. Here, we will use an approach based on positivity theory and monotonicity to study formation control on the circle.

Positivity theory plays an important role in the theory of dynamical systems with numerous applications to control engineering including stabilization [26, 27], observer design [28], and distributed control [29], as well as the modeling of biological systems [30]. Linear positive systems are systems that leave a cone invariant. According to Perron-Frobenius theory, a linear system that is strictly positive, in the sense that it maps the boundary of a pointed convex solid cone into its interior, has a dominant one-dimensional eigenspace within the cone, which asymptotically attracts all trajectories inside the cone. A natural generalization of positivity to nonlinear systems is provided by the notion of *differential positivity*, which is the property of systems whose linearization along trajectories are positive with respect to a cone field [31] and is closely related to monotonicity. Strictly differentially positive systems infinitesimally contract a cone field along trajectories, constraining the asymptotic behavior to be one-dimensional under suitable technical conditions [31, 14, 32]. See [33] for the

closely related notion of p -dominance and its applications to differential dissipativity theory.

This paper is organized as follows. In Section 2, we review the relevant results from linear positivity, consensus, and differential positivity. In Section 3, we note previous works on the topic of consensus on the circle. The node-wise monotone barrier coupling law is proposed in Section 4, where the analysis of the number and the shape of the multiple central patterns are also given. In Section 5, based on the former analysis, we investigate the viability of assigning multiple central patterns and provide the design guideline. We provide essential background on graph theory in Appendix A and present a technical lemma needed for the proof of our main result in Appendix B.

Notation: Laplacian matrix $\mathcal{L} = [l_{ij}] \in \mathbb{R}^{N \times N}$ of a graph is defined as $\mathcal{L} := \mathcal{D} - \mathcal{A}$, where $\mathcal{A} = [\alpha_{ij}]$ is the adjacency matrix of the graph and \mathcal{D} is the diagonal matrix whose diagonal entries are determined such that each row sum of \mathcal{L} is zero. By its construction, it contains at least one eigenvalue of zero, whose corresponding eigenvector is $1_N := [1, \dots, 1]^\top \in \mathbb{R}^N$, and all the other eigenvalues have non-negative real parts. For directed graphs (digraphs), the zero eigenvalue is simple if and only if the corresponding graph is connected; if it contains a directed spanning tree. For vectors or matrices a and b , $\text{col}(a, b) := [a^T, b^T]^\top$. For a set \mathcal{Z} , its cardinality is denoted by $|\mathcal{Z}|$. The function $\text{sgn} : \mathbb{R} \rightarrow \mathbb{R}$ denotes the signum function defined as $\text{sgn}(s) = s/|s|$ for non-zero s , and $\text{sgn}(s) = 0$ for $s = 0$.

2. Positivity, monotonicity, and consensus

2.1. Linear positivity and consensus

A linear system $\dot{x} = Ax$ on a vector space \mathcal{V} is said to be positive with respect to a pointed convex solid cone $\mathcal{K} \subseteq \mathcal{V}$ if $e^{At}\mathcal{K} \subseteq \mathcal{K}$, for all $t > 0$, where $e^{At}\mathcal{K} := \{e^{At}x : x \in \mathcal{K}\}$. Continuous-time linear consensus algorithms take the form $\dot{x} = A(t)x$, where $A = [a_{ij}]$ is a matrix whose rows sum to zero and whose off-diagonal elements are non-negative: $A(t)1_N = 0$, and $a_{ij} \geq 0$ for $i \neq j$. Such continuous-time linear protocols arise from dynamics of the form $\dot{x}_i = \sum_{j \in \mathcal{N}_i} a_{ij}(x_j - x_i)$ generated by N agents exchanging information via a communication graph \mathcal{G} with vertices and edges $(\mathcal{N}, \mathcal{E})$, and are strictly positive with respect to the positive orthant $\mathcal{K} := \mathbb{R}_+^N$ in \mathbb{R}^N for a strongly connected graph. The projective distance to 1_N given by the Hilbert metric of the positive orthant provides the Lyapunov function

$$V(x) = \log \frac{\max_i x_i}{\min_i x_i} = \max_i \log x_i - \min_i \log x_i,$$

which coincides with the well-known Tsitsiklis Lyapunov function in log coordinates. The Tsitsiklis Lyapunov function is non-increasing along solutions and the proof that it decreases strictly over a uniform horizon under appropriate assumptions can be established via elementary calculations [34]. The non-quadratic nature of the Tsitsiklis Lyapunov function is unavoidable. Indeed, [35] provides examples of matrices that satisfy the assumptions of a linear consensus algorithm but fail to admit a common time-invariant quadratic Lyapunov function.

2.2. Differential positivity

Differential positivity can be defined on a manifold \mathcal{M} equipped with a smooth cone field $\mathcal{K}(x) \subset T_x\mathcal{M}$. A continuous-time dynamical system Σ is said to be differentially positive with respect to \mathcal{K} if

$$d\psi_t|_x \mathcal{K}(x) \subseteq \mathcal{K}(\psi_t(x)), \quad (1)$$

for all $x \in \mathcal{M}$ and $t \geq 0$, where $\psi_t(x)$ is the flow at time t from initial condition x and $d\psi_t|_x$ denotes the differential of ψ_t at x . The definition can be extended to strict differential positivity and uniformly strict differential positivity [14].

Differential positivity provides a local characterization of monotonicity [14, 32]. A dynamical system Σ on a vector space \mathcal{V} endowed with a partial order \preceq induced by some cone $\mathcal{K} \subseteq \mathcal{V}$ is said to be monotone if for any $x_1, x_2 \in \mathcal{V}$ the trajectories ψ_t satisfy $\psi_t(x_1) \preceq_{\mathcal{K}} \psi_t(x_2)$ whenever $x_1 \preceq_{\mathcal{K}} x_2$, for all $t > 0$. If $(x(\cdot), \delta x(\cdot))$ denotes a trajectory of the prolonged or variational system $\delta\Sigma$, then Σ is monotone if and only if it is differentially positive. In other words, the system is monotone if and only if for all $t > 0$, $\delta x(0) \in \mathcal{K} \Rightarrow \delta x(t) \in \mathcal{K}$. The infinitesimal characterization suggests a natural generalization to Lie groups, requiring differential positivity with respect to an invariant cone field [14, 32].

In [31], the authors provide a generalization of Perron-Frobenius theory to nonlinear systems within a differential framework, whereby the Perron-Frobenius eigenvector of linear positivity theory is replaced by a Perron-Frobenius vector field $w(x)$ whose integral curves shape the attractors of the system. For the purposes of this paper, the characterization provided by the following theorem will suffice [36].

Theorem 1. *Let Σ be a strictly differentially positive system with respect to a cone field $\mathcal{K}(x)$ in a compact and forward invariant region $\mathcal{C} \subseteq \mathcal{M}$. If there exists a complete vector field w satisfying $w(x) \in \text{int } \mathcal{K}(x) \setminus \{0\}$ such that $\limsup_{t \rightarrow \infty} |d\psi_t|_x w(x)|_{\psi_t(x)} < \infty$, and for all $x \in \mathcal{C}$ and $t \geq 0$:*

$$w(\psi_t(x)) = \frac{d\psi_t|_x w(x)}{|d\psi_t|_x w(x)|_{\psi_t(x)}}, \quad (2)$$

then there exists an integral curve of $w(x)$ whose image is an attractor for all the trajectories of Σ from \mathcal{C} .

3. Consensus on the circle

The design of individual coupling laws to achieve asymptotic consensus on a common point in a vector space is a well-studied problem [37, 38, 39]. The analysis relies on convexity. In particular, for the real line, if each agent moves toward a strict inner point of the convex hull of the values of its neighbors, then the minimal (maximal) value among all the agents can only increase (decrease) until they become equal.

On nonlinear spaces, this argument, relying on convexity, cannot be used globally. In particular, for multiple agents on the circle, there is no ‘minimal’ or ‘maximal.’ The convexity argument applies only when all agents are initially placed within a semi-circle [40, 38]. In this respect, a number of papers have considered the construction of local controllers to achieve (almost) global convergence properties. In particular, modified Kuramoto coupling, Gossip algorithm, and hybrid coupling have been proposed.

Meanwhile, to the best of our knowledge, these works either apply to particular interconnection topologies, like trees and all-to-all interconnection [41, 12, 16], use auxiliary variables in the embedding space [42, 12, 16], use global information such as the number of agents N [43], can lead to unnecessarily slow convergence rates [44], or are only analyzed for two agents [45].

4. Node-wise monotone barrier coupling law

As indicated in Section 3, global convergence properties are hard to achieve in general for the problem of consensus (or formation control) on the circle, unless the control is stochastic. In other words, in general, there are multiple steady-state behaviors or even chaotic ones. From an engineering viewpoint, this issue can be resolved, if we have our control on the multiple central patterns and their associated domain of attraction. For this purpose, we introduce a barrier effect in our coupling, motivated by our initial work [24], to partition the state space into finite regions, where for each partition there exists a unique steady-state behavior.

In particular, for a given interaction topology $\mathcal{G} = (\mathcal{N}, \mathcal{E})$, $\mathcal{N} := \{1, \dots, N\}$ and ‘intrinsic’ frequencies $\omega_i \in \mathbb{R}$, $i \in \mathcal{N}$, we consider the *node-wise monotone barrier coupling law* for a group of N agents evolving on the circle \mathbb{S}^1 as

$$\dot{\theta}_i = \omega_i + f_i(\nu_i + \phi_i), \quad \nu_i = \sum_{j \in \mathcal{N}_i} \alpha_{ij}(\theta_j - \theta_i), \quad (3)$$

where $\theta_i \in \mathbb{S}^1$ represents the phase of agent i , \mathcal{N}_i is a subset of \mathcal{N} whose elements are indices of the agents that send information to agent i (hence $\mathcal{E} \equiv \{(j, i) : j \in \mathcal{N}_i, i \in \mathcal{N}\}$), and f_i denotes a coupling function on the domain $(-\pi, \pi)$ extended to \mathbb{R} , 2π -periodically. The interconnection weights $\alpha_{ij} > 0$ and the phase biases $\phi_i \in (-\pi, \pi)$ are the design parameters. Note that for the coupling to be well-defined for $\theta_i \in \mathbb{S}^1$, we should have $\alpha_{ij} \in \mathbb{N}$; that is the network should be quantized. Let $\theta = (\theta_1, \dots, \theta_N)$ denote an element of the N -torus \mathbb{T}^N and consider the N -tuple of vector fields $(\frac{\partial}{\partial \theta^1}, \dots, \frac{\partial}{\partial \theta^N})$, which defines a basis vector fields on \mathbb{T}^N . Assuming that the coupling functions f_i are differentiable and strictly monotonically increasing on $(-\pi, \pi)$, then it can be shown that the linearization $\delta\dot{\theta} = A(\theta)\delta\theta$ of the system given by (3) is uniformly strictly differentially positive on the set $\mathbb{T}_\pi^N = \{\theta \in \mathbb{T}^N : |\nu_i + \phi_i| \neq \pi \bmod 2\pi, i \in \mathcal{N}\}$ with respect to the cone field

$$\mathcal{K}_{\mathbb{T}^N}(\theta) := \left\{ \delta\theta \in T_\theta \mathbb{T}^N : \delta\theta^i \geq 0, \delta\theta = \sum_i \delta\theta^i \frac{\partial}{\partial \theta^i} \right\},$$

for any strongly connected communication graph \mathcal{G} . Furthermore, the Perron-Frobenius vector field of the system on \mathbb{T}_π^N is the left-invariant vector field $1_N(\theta) = (1, \dots, 1) \in T_\theta \mathbb{T}^N$, where the vector representation is given with respect to the basis defined by $(\frac{\partial}{\partial \theta^1}, \dots, \frac{\partial}{\partial \theta^N})$. Moreover, if we denote the flow of (3) by ψ_t , then the condition $A(\theta)1_N(\theta) = 0$ implies that $d\psi_t|_\theta 1_N(\theta) = 1_N(\psi_t(\theta))$, which ensures that $\limsup_{t \rightarrow \infty} |d\psi_t|_\theta 1_N(\theta)|_{\psi_t(\theta)} < \infty$ for any flow confined to \mathbb{T}_π^N . If we add the requirement that the coupling functions f_i be barrier functions on $(-\pi, \pi)$ so that $f_i(s) \rightarrow \pm\infty$ as $s \rightarrow \pm\pi$, then the flow ψ_t will be forward invariant on \mathbb{T}_π^N , under the following assumption.

Assumption 1. The communication graph \mathcal{G} is connected; \mathcal{G} contains a spanning tree.

Theorem 2. Under Assumption 1, consider a network of agents on \mathbb{S}^1 communicating according to (3). If the coupling functions f_i satisfy $f_i(s) \rightarrow \pm\infty$ as $s \rightarrow \pm\infty$, then every trajectory starting from \mathbb{T}_π^N resides inside \mathbb{T}_π^N . Moreover, the trajectory converges to an integral curve of the vector field $1_N = 1_N(\theta)$. Finally, for each trajectory, the control input $f_i(\nu_i(t) + \phi_i)$ is bounded uniformly on $[0, \infty)$.

Remark 1. Convergence to an integral curve of 1_N on \mathbb{T}_π^N corresponds to phase-locking behavior, whereby the collective motion asymptotically converges to movement in a fixed formation with frequency synchronization among the agents. Further details may be found in [14].

In the following sections, we will further investigate

- the shape of the steady-state behavior,
- the number of different steady-state behaviors,
- what shapes can be assigned,
- and how to achieve them.

We neglect analysis of the convergence rate as it depends on the slope of our coupling functions $f_i(\cdot)$, and thus, can be increased arbitrarily large.

4.1. Generated central patterns on the circle

Coupling functions that ensure forward invariance of the consensus dynamics in \mathbb{T}_π^N generally split the torus into a finite number of disconnected components defined by the barrier functions and the communication graph topology. Given almost any initial configuration on the torus, the trajectory is attracted to a pattern that is unique to the particular disconnected component corresponding to the initialization. For a fixed given set of intrinsic frequencies $\{\omega_i\}_{\mathcal{N}}$, a set of coupling functions $\{f_i(\cdot)\}_{\mathcal{N}}$, a set of interconnection weights $\{\alpha_{ij}\}_{\mathcal{E}} \in \mathbb{N}$, and a set of phase biases $\{\phi_i\}_{\mathcal{N}}$, we can identify a formation that the network (3) asymptotically converges to, which depends on the initial condition.

In particular, if we realize the N -torus \mathbb{T}^N by $(-\pi, \pi)^N$, then the coupling functions that ensure forward invariance of the consensus dynamics in \mathbb{T}_π^N guarantees that the solution trajectory starting from each partition of $(-\pi, \pi)^N$ given as

$$\Theta_{\{n_i\}_{\mathcal{N}}} := \{\theta \in (-\pi, \pi)^N \mid \nu_i + \phi_i - 2n_i\pi \in (-\pi, \pi)\},$$

for each $\{n_i\}_{\mathcal{N}} \in \mathbb{N}$, remains inside

$$\Theta_{\{n_i\}_{\mathcal{N}}}^{\mathbb{R}} := \{\theta \in \mathbb{R}^N \mid \nu_i + \phi_i - 2n_i\pi \in (-\pi, \pi)\},$$

for all future time. Note that the number of sequences $\{n_i\}_{\mathcal{N}} \in \mathbb{Z}$ such that $\Theta_{\{n_i\}_{\mathcal{N}}} \neq \emptyset$ is finite. In particular, we should have $n_i \in [-d_i, d_i]$, where $0 \leq d_i = \sum_{j \in \mathcal{N}_i} \alpha_{ij} \in \mathbb{Z}$, and thus, the number is upper bounded by $\prod_{i \in \mathcal{N}} (2d_i + 1)$.

Now, for the trajectories starting from $\Theta_{\{n_i\}_{\mathcal{N}}}$, we can find a unique shape; a common frequency $\bar{\omega}$ and a formation $\{\Delta_{ij}\}_{\mathcal{E}} \in (-\pi, \pi)$ (i.e., a phase difference given for each edge), that it converges to, which should satisfy

$$\bar{\omega} = \omega_i + f_i \left(\sum_{j \in \mathcal{N}_i} \alpha_{ij} \Delta_{ij} + \phi_i \right), \quad i \in \mathcal{N}. \quad (4)$$

For this purpose, note first that the formation $\{\Delta_{ij}\}_{\mathcal{E}}$ must be generated, for instance, by the collection of fixed phases $\{\Delta_i\}_{\mathcal{N}} \in \mathbb{R}$ that satisfies $\text{col}(\Delta_1, \dots, \Delta_N) \in \Theta_{\{n_i\}_{\mathcal{N}}}^{\mathbb{R}}$ and $\Delta_1 = 0$, as $\Delta_{ij} = \Delta_j - \Delta_i \bmod 2\pi$. This is because of forward invariance. Utilizing this fact, (4) can be written otherwise as

$$\bar{\omega} = \omega_i + f_i \left(\sum_{j \in \mathcal{N}_i} \alpha_{ij} (\Delta_j - \Delta_i) + \phi_i \right), \quad i \in \mathcal{N}.$$

This implies

$$\sum_{j \in \mathcal{N}_i} \alpha_{ij} (\Delta_j - \Delta_i) + \phi_i = f_i^{-1}(\bar{\omega} - \omega_i) + 2n_i\pi,$$

where the inverse f_i^{-1} is defined as a mapping from \mathbb{R} into $(-\pi, \pi)$. Hence, by the identity

$$\sum_{i \in \mathcal{S}} \zeta_i \sum_{j \in \mathcal{N}_i} \alpha_{ij} (\Delta_j - \Delta_i) = 0,$$

where \mathcal{S} denotes the unique independent strongly connected component (iSCC)¹ and $\zeta_i > 0$, $i \in \mathcal{S}$ are the components of the left eigenvector of \mathcal{L} associated with the zero eigenvalue, i.e., $[\zeta_1 \ \dots \ \zeta_N] \mathcal{L} = 0$,² we get

$$F(\bar{\omega}) := \sum_{i \in \mathcal{S}} \zeta_i (f_i^{-1}(\bar{\omega} - \omega_i) + 2n_i\pi - \phi_i) = 0. \quad (5)$$

Since the function $F : \mathbb{R} \rightarrow \mathbb{R}$ is continuous and strictly increasing with respect to $\bar{\omega}$, and satisfies $\lim_{\bar{\omega} \rightarrow \pm\infty} F(\bar{\omega}) \rightarrow \sum_{i \in \mathcal{S}} \zeta_i (\pm\pi + 2n_i\pi - \phi_i)$, where³

$$-\sum_{i \in \mathcal{S}} \zeta_i \pi < \sum_{i \in \mathcal{S}} \zeta_i (2n_i\pi - \phi_i) < \sum_{i \in \mathcal{S}} \zeta_i \pi, \quad (6)$$

we have the existence and the uniqueness of the solution $\bar{\omega}$ of (5). With this unique $\bar{\omega}$, we have our unique formation $\{\Delta_i\}_{\mathcal{N}}$ given by

$$-\mathcal{L} \begin{bmatrix} \Delta_1 \\ \vdots \\ \Delta_N \end{bmatrix} = \begin{bmatrix} f_1^{-1}(\bar{\omega} - \omega_1) + 2n_1\pi - \phi_1 \\ \vdots \\ f_N^{-1}(\bar{\omega} - \omega_N) + 2n_N\pi - \phi_N \end{bmatrix}. \quad (7)$$

Note that the Laplacian matrix \mathcal{L} has rank $N - 1$, but we also have $N - 1$ dimensions for the configuration space of $\text{col}(\Delta_1, \dots, \Delta_N) \in \Theta_{\{n_i\}_{\mathcal{N}}}^{\mathbb{R}}$ from the constraint $\Delta_1 = 0$ we posed earlier, hence $\{\Delta_i\}_{\mathcal{N}}$ uniquely exists. This uniquely defines the edge-wise formation $\{\Delta_{ij}\}_{\mathcal{E}} \in (-\pi, \pi)$, by the relation $\Delta_{ij} = \Delta_j - \Delta_i \bmod 2\pi$.

Remark 2. Here, we can see the resiliency of the generated patterns with respect to individual variability. In particular, $f_i^{-1}(\cdot)$ is a sigmoidal function, and thus, equation (5) rejects outliers ω_i , as done by the median in statistics, which is the solution of the similar equation

$$\sum_{i=1}^N \text{sgn}(\bar{\omega} - \omega_i) = 0.$$

In general, $\bar{\omega}$ becomes more tolerant to ω_i which is largely departed. This is also for the formation, as can be seen in (7).

¹It is well-known that a graph which contains a spanning tree has exactly one iSCC (independent Strongly Connected Component).

²By its definition, we have $\zeta_i = 0$ for all $i \in \mathcal{N} \setminus \mathcal{S}$.

³Since $\Theta_{\{n_i\}_{\mathcal{N}}} \neq \emptyset$, there exists $\theta \in \Theta_{\{n_i\}_{\mathcal{N}}}$ such that $\nu_i + \phi_i - 2n_i\pi =: \psi_i \in (-\pi, \pi)$, $i \in \mathcal{N}$, we get $\sum_{i \in \mathcal{S}} \zeta_i (2n_i\pi - \phi_i) = \sum_{i \in \mathcal{S}} \zeta_i (\nu_i - \psi_i) = -\sum_{i \in \mathcal{S}} \zeta_i \psi_i$. This implies (6).

4.2. Number of different central patterns

On top of the discussions made in Section 4.1, we want to point out that two shapes $(\bar{\omega}^1, \{\Delta_{ij}^1\}_{\mathcal{E}})$ and $(\bar{\omega}^2, \{\Delta_{ij}^2\}_{\mathcal{E}})$ associated with two different sequences $\{n_i^1\}_{\mathcal{N}} \in \mathbb{Z}$ and $\{n_i^2\}_{\mathcal{N}} \in \mathbb{Z}$ might coincide. The necessary and sufficient condition for this case is

- $\sum_{i \in \mathcal{S}} \zeta_i n_i^1 = \sum_{i \in \mathcal{S}} \zeta_i n_i^2$
- and that the corresponding solutions $\{\Delta_i^1\}$ and $\{\Delta_i^2\}$ satisfy $\Delta_i^1 = \Delta_i^2 \pmod{2\pi}$ for all $i \in \mathcal{N}$.

This is because, for different $\sum_{i \in \mathcal{S}} \zeta_i n_i$, we have different $\bar{\omega}$, since $\sum_{i \in \mathcal{S}} \zeta_i f_i^{-1}(\bar{\omega} - \omega_i)$ in (5) is strictly increasing. The second condition is equivalent to the condition that the equation $(\Delta_i^1 - \Delta_i^2 = 2\tilde{\delta}_i \pi)$

$$-\mathcal{L} \begin{bmatrix} 0 \\ \tilde{\delta}_2 \\ \vdots \\ \tilde{\delta}_N \end{bmatrix} = \begin{bmatrix} n_1^1 - n_1^2 \\ n_2^1 - n_2^2 \\ \vdots \\ n_N^1 - n_N^2 \end{bmatrix}$$

has a unique integer solution $\tilde{\delta}_2, \dots, \tilde{\delta}_N$, or equivalently that the vector in the right-hand side being spanned by the columns of the Laplacian matrix with integer-valued weights. So, let us define an equivalence relation for two sequences if and only if the above relation, that $\sum_{i \in \mathcal{S}} \zeta_i n_i^1 = \sum_{i \in \mathcal{S}} \zeta_i n_i^2$ and that there exists a unique integer solution $\tilde{\delta}_2, \dots, \tilde{\delta}_N$, is satisfied, and denote it as $\{n_i^1\}_{\mathcal{N}} \sim \{n_i^2\}_{\mathcal{N}}$. We also denote the equivalence class as $[\{n_i^1\}_{\mathcal{N}}]$.

Then, the number of different shapes $(\bar{\omega}, \{\Delta_{ij}\}_{\mathcal{E}})$ of the network (3) depending on the initial condition can be fully characterized by a graph theoretical interpretation as the number of different equivalence classes $[\{n_i\}_{\mathcal{N}}]$ such that there exists $\{n_i\}_{\mathcal{N}} \in [\{n_i\}_{\mathcal{N}}]$ satisfying $\Theta_{\{n_i\}_{\mathcal{N}}} \neq \emptyset$.

Remark 3. *On the other hand, the number of different $\sum_{i \in \mathcal{S}} \zeta_i n_i =: n_{\mathcal{S}}$ is straightforward. In particular, the left eigenvector of \mathcal{L} associated with the zero eigenvalue can always be taken as an integer vector where the common denominator of the components is 1.⁴ Then, the number of different $n_{\mathcal{S}}$ is simply upper bounded by $\sum_{i \in \mathcal{S}} \zeta_i =: \zeta_{\mathcal{S}}$ or $\zeta_{\mathcal{S}} - 1$. This is because, we have from $\nu_i + \phi_i - 2n_i \pi \in (-\pi, \pi)$ that*

$$\sum_{i \in \mathcal{S}} \zeta_i \phi_i - 2n_{\mathcal{S}} \pi \in (-\zeta_{\mathcal{S}} \pi, \zeta_{\mathcal{S}} \pi),$$

hence for each $\phi_{\mathcal{S}} = \sum_{i \in \mathcal{S}} \zeta_i \phi_i$, we get

$$n_{\mathcal{S}} \in \left(-\frac{\zeta_{\mathcal{S}}}{2} + \frac{\phi_{\mathcal{S}}}{2\pi}, \frac{\zeta_{\mathcal{S}}}{2} + \frac{\phi_{\mathcal{S}}}{2\pi} \right).$$

4.3. Further discussions

The characterization of equivalence relation can be divided for the two index sets each associated with the unique iSCC, \mathcal{S} , and the followers, $\mathcal{N} \setminus \mathcal{S}$. In particular, two sequences are equivalent $\{n_i^1\}_{\mathcal{N}} \sim \{n_i^2\}_{\mathcal{N}}$ if and only if

⁴This is because, $\mathcal{L} - 0I$ is integer-valued, and thus, Gaussian elimination will produce rational eigenvectors.

- $\{n_i^1\}_{\mathcal{S}} \sim \{n_i^2\}_{\mathcal{S}}$

- and $\sum_{j \in \mathcal{N}_i} \alpha_{ij} (\tilde{\delta}_j - \tilde{\delta}_i) = n_i^1 - n_i^2$ for all $i \in \mathcal{N} \setminus \mathcal{S}$.

The second condition can be made independent of the $\tilde{\delta}_i$, $i \in \mathcal{S}$, by first characterizing all admissible integer sequences $\{\tilde{n}_i\}_{\mathcal{N} \setminus \mathcal{S}} \in \mathbb{Z}$ that can be generated by $\{\tilde{\delta}_i\}_{\mathcal{N} \setminus \mathcal{S}} \in \mathbb{Z}$ as

$$\sum_{j \in \mathcal{N}_i \cap \mathcal{N} \setminus \mathcal{S}} \alpha_{ij} \tilde{\delta}_j - \sum_{j \in \mathcal{N}_i} \alpha_{ij} \tilde{\delta}_i = \tilde{n}_i, \quad i \in \mathcal{N} \setminus \mathcal{S},$$

then letting

$$\tilde{n}_i = n_i^1 - n_i^2 - \sum_{j \in \mathcal{N}_i \cap \mathcal{S}} \alpha_{ij} \tilde{\delta}_j, \quad i \in \mathcal{N} \setminus \mathcal{S},$$

for each equivalence relation $\{n_i^1\}_{\mathcal{S}} \sim \{n_i^2\}_{\mathcal{S}}$. In particular, if all the followers have only one neighbor, $|\mathcal{N}_i| = 1$, and $\alpha_{ij} = 1$, $j \in \mathcal{N}_i$, then $\{n_i^1\}_{\mathcal{N}} \sim \{n_i^2\}_{\mathcal{N}}$ if and only if $\{n_i^1\}_{\mathcal{S}} \sim \{n_i^2\}_{\mathcal{S}}$. This is because there is no loop in graph $(\mathcal{N} \setminus \mathcal{S}, \mathcal{E}|_{\mathcal{N} \setminus \mathcal{S}})$. This can be also seen by considering \mathcal{S} as a single node, which makes the new graph a spanning tree.

However, in general, the equivalence relation defined in Section 4.2 is complicated, and the fact that α_{ij} is an integer gives an additional restriction via the equality

$$\sum_{j \in \mathcal{N}_i} \alpha_{ij} (\tilde{\delta}_j - \tilde{\delta}_i) = n_i^1 - n_i^2, \quad i \in \mathcal{N},$$

and it is most likely that different $\{n_i\}_{\mathcal{N}}$ are not equivalent. In this sense, making $\alpha_{ij} = 1$ for all $(j, i) \in \mathcal{E}$ tends to reduce the number of different shapes. This is because the number of admissible $\{n_i\}_{\mathcal{N}}$ ($\Theta_{\{n_i\}_{\mathcal{N}}} \neq \emptyset$) reduces. In particular, the upper bound $\prod_{i \in \mathcal{N}} (2d_i + 1)$ reduces.

On the other hand, a strongly connected graph that ensures that two sequences $\{n_i^1\}_{\mathcal{N}}$ and $\{n_i^2\}_{\mathcal{N}}$ are equivalent if and only if $\sum_{i \in \mathcal{N}} \zeta_i n_i^1 = \sum_{i \in \mathcal{N}} \zeta_i n_i^2$, generically has the following form of Laplacian matrix.

$$\mathcal{L} = \begin{bmatrix} 1 & -1 & & & & \\ * & * & -1 & & & \\ \vdots & \vdots & \vdots & \ddots & & \\ * & * & * & \cdots & -1 & \\ * & * & * & * & * & * \end{bmatrix}$$

This includes the cases of directed ring graphs and undirected line graphs, which have 1_N as the left eigenvector associated with the zero eigenvalue, resulting in N or $N-1$ different central patterns (Remark 3).

Further studies might be on the general graph theoretical characterization of the exact number of different equivalence classes. For this purpose, the integer-valued Laplacian matrix should be studied in depth. Meanwhile, such a number can always be obtained by numerical computation.

Remark 4. *If we cut the barrier function at a finite region, that is $f_i : (-\pi, \pi) \rightarrow (M_i^-, M_i^+)$ with some $M_i^- < M_i^+$ but f_i is still strictly increasing and satisfies $\lim_{s \rightarrow \pm\pi} f_i(s) = M_i^{\pm}$, then since the monotonicity is preserved, the behavior of the network will be either converging to some shape and achieving phase-locking behavior or moving to the discontinuous boundary. In particular, if we saturate the original barrier function to $[M_i^- + \delta, M_i^+ - \delta]$,*

and then for the saturated region perform an arbitrary small perturbation so that the resulting function is still strictly increasing, then there are no new central patterns generated, and thus, for those shapes $(\bar{\omega}, \{\Delta_{ij}\}_{\mathcal{E}})$ outside the saturated region; for those which has $i \in \mathcal{N}$ such that $\bar{\omega} - \omega_i \notin (M_i^-, M_i^+)$, the trajectory moves to the boundary.⁵ Then, depending on the vector field on the opposite side, it either moves to another region associated with another sequence $\{n_i\}_{\mathcal{N}}$ in a finite time or stays on the boundary. In other words, if we set M_i^- and M_i^+ for each $i \in \mathcal{N}$ such that $\bar{\omega} - \omega_i \in (M_i^-, M_i^+)$ for all shapes $(\bar{\omega}, \{\Delta_{ij}\}_{\mathcal{E}})$, then the original behavior will be mostly maintained, while some might converge to the boundary and stay there.

5. Assigning central patterns in the network

5.1. Viability of assigning one central pattern

Now, we consider the problem of shaping consensus; given a digraph $\mathcal{G} = (\mathcal{N}, \mathcal{E})$, a set of intrinsic frequencies $\{\omega_i\}_{\mathcal{N}}$, a common frequency $\bar{\omega}$, and a formation $\{\Delta_{ij}\}_{\mathcal{E}}$, find

- a set of interconnection weights $\{\alpha_{ij}\}_{\mathcal{E}}$,
- a set of phase biases $\{\phi_i\}_{\mathcal{N}}$,
- and a set of coupling functions $\{f_i(\cdot)\}_{\mathcal{N}}$,

such that the given shape $(\bar{\omega}, \{\Delta_{ij}\}_{\mathcal{E}})$ represents a phase-locking behavior governed by the equation (4) that the network (3) achieves.

Note first that if we only have freedom to choose the interconnection weights $\{\alpha_{ij}\}_{\mathcal{E}} \in \mathbb{N}$, then, in principle, it is impossible to solve the problem. This is because

$$\begin{bmatrix} f_1 \left(\sum_{j \in \mathcal{N}_1} \alpha_{1j} \Delta_{1j} + \phi_1 \right) \\ \vdots \\ f_N \left(\sum_{j \in \mathcal{N}_N} \alpha_{Nj} \Delta_{Nj} + \phi_N \right) \end{bmatrix}$$

forms only a measure zero set in \mathbb{R}^N .

On the other hand, if we have freedom of choice for either the set of coupling functions $\{f_i\}$ or the set of phase biases $\{\phi_i\}$, then the problem is always solvable because given any shape, we can always find $\{f_i\}$ or $\{\phi_i\}$ such that

$$f_i \left(\sum_{j \in \mathcal{N}_i} \alpha_{ij} \Delta_{ij} + \phi_i \right) = \bar{\omega} - \omega_i, \quad i \in \mathcal{N},$$

from the fact that $f_i, i \in \mathcal{N}$, are barrier functions.

If we restrict our coupling functions to be the scaled version of a single function, i.e., $f_i(\cdot) = g_i \bar{f}(\cdot)$ with positive coefficients g_i ,⁶ then the problem of finding an appropriate set of coupling functions becomes algebraic. However, in this case, the problem is solvable if and only if

$$\operatorname{sgn} \left(\bar{f} \left(\sum_{j \in \mathcal{N}_i} \alpha_{ij} \Delta_{ij} + \phi_i \right) \right) = \operatorname{sgn} (\bar{\omega} - \omega_i), \quad i \in \mathcal{N}. \quad (8)$$

This can always be satisfied if we have freedom of choice with respect to the phase biases. Otherwise, if we only have freedom of choice for the interconnection weights, then we can always satisfy (8) provided $\bar{\omega} \neq \omega_i$ and

- there exists $j \in \mathcal{N}_i$ such that $\Delta_{ij}/(2\pi)$ is an irrational number.

If we also restrict the interconnection weights to take a prototypical ratio, i.e., $\alpha_{ij} = \beta_i \bar{\alpha}_{ij}$ with positive integers β_i , then we can always satisfy (8) if $\bar{\omega} \neq \omega_i$ and

- $\bar{\Delta}_i := \sum_{j \in \mathcal{N}_i} \bar{\alpha}_{ij} \Delta_{ij}$ satisfy that $\bar{\Delta}_i/(2\pi)$ is an irrational number.

Note that given a formation $\{\Delta_{ij}\}_{\mathcal{E}}$, we can always perform an arbitrarily small perturbation so that the above irrational number condition is satisfied, hence we can achieve our design goal with arbitrary precision. In particular, in the former case, we can even select an arbitrary edge to satisfy that $\Delta_{ij}/(2\pi)$ is an irrational number. This is because, any formation $\{\Delta_{ij}\}_{\mathcal{E}}$ is generated by a sequence of phases $\{\Delta_i\}_{\mathcal{N}} \in (-\pi, \pi)$ as $\Delta_{ij} = \Delta_j - \Delta_i$, and thus, with any irrational number r , if we perturb $\{\Delta_i\}_{\mathcal{N}}$ as $\tilde{\Delta}_i = \Delta_i + (\epsilon \cdot i \cdot r)2\pi, i \in \mathcal{N}$, then for almost all sufficiently small rational numbers ϵ , $\Delta_{ij}/(2\pi)$ becomes irrational.

Remark 5. *Coupling functions having a prototypical shape, i.e., $f_i(\cdot) = g_i \bar{f}(\cdot)$, coincide with the philosophy of CPGs, where the central patterns are designed by the maximal conductances g_i of the synaptic coupling $g_i \bar{f}(\cdot)$ [18].*

5.2. Design guideline for a minimal number of connections

Among all of the possible choices we could take for assigning a central pattern, we provide a design guideline that maximizes the number of interconnection weights that we can set to zero, given a digraph $\mathcal{G} = (\mathcal{N}, \mathcal{E})$.

If we have freedom of choice with respect to either the set of coupling functions or the set of phase biases, then according to Section 5.1, we can simply choose our interconnection weights so that the reduced subgraph (governed by positive weights) still contains a spanning tree. In particular, we can simply make the number of interconnections as $N - 1$, by picking one root node from the unique iSCC of the original graph, and then taking any spanning tree.

If we consider the scaled version of coupling functions, then such subgraphs should include those edges (j, i) such that $\Delta_{ij}/(2\pi)$ is an irrational number for each $i \in \mathcal{N}$; for each $i \in \mathcal{N}$, there exists at least one positive interconnection weight α_{ij} . Then, by denoting such a set of edges as $\mathcal{E}' \subset \mathcal{E}$, the corresponding least communication subgraph, which contains \mathcal{E}' , can be found as follows.

1. Consider the reduced graph $\mathcal{G}'_{\mathcal{S}} = (\mathcal{S}, \mathcal{E}'|_{\mathcal{S}})$. Add a minimum number of edges so that the new reduced graph $(\mathcal{S}, \mathcal{E}_{\mathcal{S}})$ contains a spanning tree. This can be done as follows.
 - (a) The reduced graph $\mathcal{G}'_{\mathcal{S}}$ consists of its iSCCs and followers. Consider each iSCC and its followers as a single node (a follower can be included in multiple nodes), and define an edge from one node to another if there is an edge in the original edge set \mathcal{E} from any agent inside one node to any agent in the iSCC of another node.
 - (b) This new graph is strongly connected. So, take any spanning tree of it and add one corresponding edge from the original edge set \mathcal{E} .

⁵This becomes clear if we observe the dynamics of $x_i := \nu_i + \phi_i$.

⁶The coefficients must be positive to ensure differential positivity.

2. Then, include all other edges in \mathcal{E}' , and add a minimum number of edges so that the new subgraph $(\mathcal{N}, \mathcal{E}_N)$ contains a spanning tree. This can be done as follows.

- (a) The graph obtained by including all other edges in \mathcal{E}' consists of its iSCCs and followers. By construction, there exists unique iSCC included in \mathcal{S} .
- (b) Now, consider the iSCC included in \mathcal{S} and its followers as a single node and consider all other iSCCs each as a single node, and define a graph according to the edge set \mathcal{E} .
- (c) Then, this new graph contains a spanning tree which has its root as the node that corresponds to the iSCC included in \mathcal{S} . Take this spanning tree and add one corresponding edge from the original edge set \mathcal{E} .

Example 1. Let's take an example for the above procedure. For this purpose, let us consider a graph $(\mathcal{N}, \mathcal{E})$ with $\mathcal{N} = \{1, \dots, 8\}$ and \mathcal{E} with $(j, i) \in \mathcal{E}$ represented by $j \rightarrow i$ in Figure 1. If the formation $\{\Delta_{ij}\}_{\mathcal{E}}$ is governed by $\Delta_{ij} = \Delta_j - \Delta_i \bmod 2\pi$ from $\{\Delta_i\}_{\mathcal{N}}$ given as

$$\begin{aligned} \Delta_1 = 0, \quad \Delta_2 = -1/50, \quad \Delta_3 = \pi/4, \quad \Delta_4 = \pi/2, \\ \Delta_5 = 3\pi/4, \quad \Delta_6 = \pi + 1/100, \quad \Delta_7 = 5\pi/4 + 1/100, \\ \Delta_8 = 3\pi/2, \quad \Delta_9 = 7\pi/4, \end{aligned}$$

then the set \mathcal{E}' and the set of edges $(j, i) \in \mathcal{E}$ such that $\Delta_{ij}/(2\pi)$ is an irrational number are obtained as in Figure 1. The procedure described above is illustrated in Figure 1.

Meanwhile, note that as illustrated in Section 5.1, we can perturb the formation infinitesimally small to select \mathcal{E}' as whatever we want. In this sense, we can make the number of interconnections smaller than or equal to N . In particular, as before, we can simply select a spanning tree, if there exists $i \in \mathcal{S}$ such that

$$\text{sgn}(\bar{f}(\phi_i)) = \text{sgn}(\bar{\omega} - \omega_i),$$

or if not, then select a spanning tree and an additional edge (j, i) for the root node i .

5.3. Design guideline for a minimal number of different shapes

Note that according to the discussions made in Section 4.3, when we choose our non-negative interconnection weights to be such that the reduced subgraph governed by positive weights is a spanning tree and those positive weights are unity, then our shape becomes unique and we have almost global convergence. This is because all of the followers have only one neighbor and $\alpha_{ij} = 1$, $j \in \mathcal{N}_i$, hence $\{n_i^1\}_{\mathcal{N}} \sim \{n_i^2\}_{\mathcal{N}}$ if and only if $\{n_i^1\}_{\mathcal{S}} \sim \{n_i^2\}_{\mathcal{S}}$. Note that \mathcal{S} is a singleton $\{i\}$, hence $\{n_i^1\}_{\mathcal{S}} \sim \{n_i^2\}_{\mathcal{S}}$ if and only if $n_i^1 = n_i^2$. Since $\nu_i \equiv 0$, any admissible $\{n_i\}_{\mathcal{N}}$ ($\Theta_{\{n_i\}_{\mathcal{N}}} \neq \emptyset$) gives $n_i = 0$; the number of different shapes is one.

In this manner, if we have freedom of choice with respect to either the set of coupling functions or the set of phase biases, then as in Section 5.2, we can simply choose

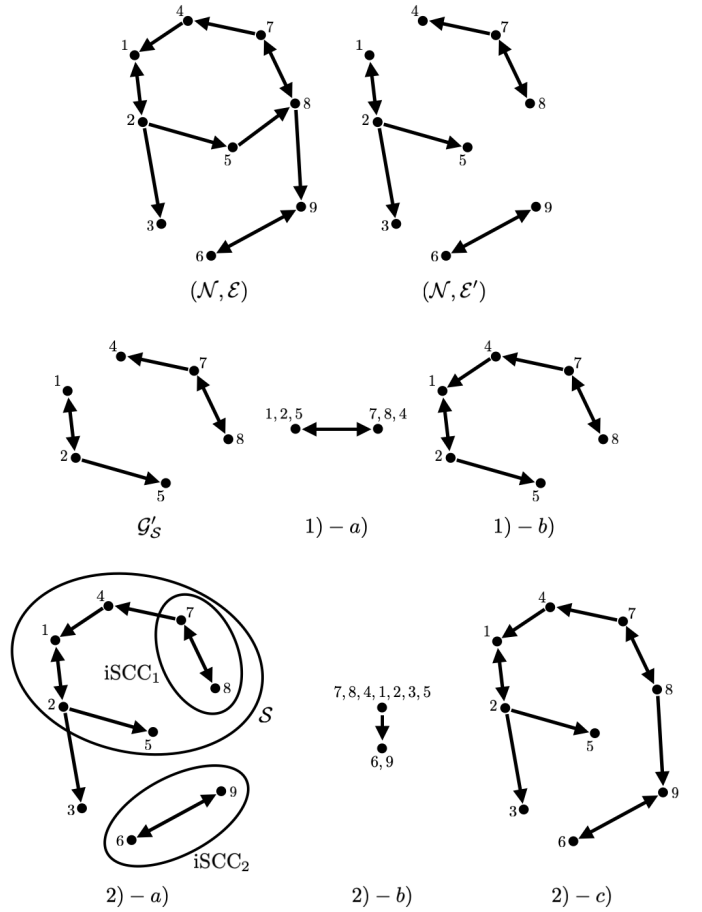


Figure 1: Illustration of the graphs $(\mathcal{N}, \mathcal{E})$ and $(\mathcal{N}, \mathcal{E}')$, and the process 1) and 2) in obtaining the least communication subgraph in Example 1.

our interconnection weights so that the reduced subgraph is a spanning tree.

On the other hand, if we restrict our coupling functions to have a prototypical shape, then in principle, α_{ij} becomes a large integer and so the number of different shapes becomes large. Meanwhile, if we have a large number of neighbors for each agent, and the formation is uniformly distributed, then we have a better chance of decreasing the number. But, in general, finding a set of interconnection weights that gives a minimal number of different shapes under the restriction on our coupling functions is a hard problem. The best we could do is to reduce the number of neighbors and to reduce the interconnection weights.

Remark 6. According to Remark 4, if we have chosen our interconnection weights, coupling functions, and phase biases, then we can simply saturate our coupling functions to a finite region (M_i^-, M_i^+) , to satisfy $\bar{\omega} - \omega_i \in (M_i^-, M_i^+)$, $i \in \mathcal{N}$ only for the desired shapes. This increases the chance to yield almost global convergence, even under the restriction $f_i = g_i \bar{f}$. The trajectory might converge to the boundary and stay, but we can always give a kick to make it converge to the desired shape.

5.4. Further discussions on Example 1

In this subsection, we follow Example 1. But, instead we consider an infinitesimal perturbation on the given formation, so that we can choose the set \mathcal{E}' of edges $(j, i) \in \mathcal{E}$ such that $\Delta_{ij}/(2\pi)$ is an irrational number, which yields the graph represented in Figure 2, a spanning tree with one

additional edge. This is achieved for the formation $\{\tilde{\Delta}_{ij}\}_{\mathcal{E}}$ governed by $\tilde{\Delta}_{ij} = \tilde{\Delta}_j - \tilde{\Delta}_i \bmod 2\pi$ from $\{\tilde{\Delta}_i\}_{\mathcal{N}}$ given as

$$\begin{aligned}\tilde{\Delta}_1 &= 0, & \tilde{\Delta}_2 &= -1/50, & \tilde{\Delta}_3 &= \pi/4, & \tilde{\Delta}_4 &= \pi/2, \\ \tilde{\Delta}_5 &= 3\pi/4, & \tilde{\Delta}_6 &= \pi + 1/50, & \tilde{\Delta}_7 &= 5\pi/4 + 1/100, \\ \tilde{\Delta}_8 &= 3\pi/2 + 1/50, & \tilde{\Delta}_9 &= 7\pi/4 + 1/100.\end{aligned}$$

Note that the only difference is $\tilde{\Delta}_6$, $\tilde{\Delta}_8$, and $\tilde{\Delta}_9$, and the difference is smaller than $1/50$.

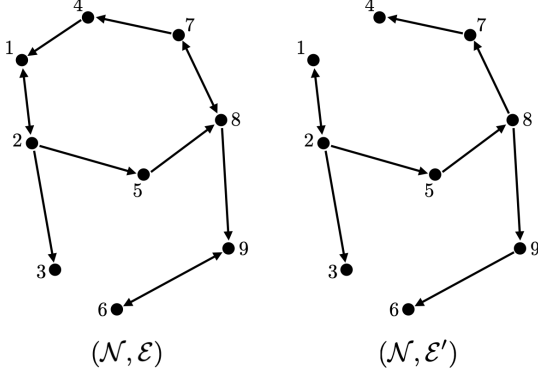


Figure 2: Illustration of the graphs $(\mathcal{N}, \mathcal{E})$ and $(\mathcal{N}, \mathcal{E}')$ in Section 5.4.

Now, consider the situation where our objective shape is determined by the above given phases $\{\tilde{\Delta}_i\}_{\mathcal{N}}$ and a common frequency $\bar{\omega} = 1$, while given that the intrinsic frequencies are $\omega_1 = 0$ and $\omega_i = 2$ for $i \neq 1$. Moreover, say our coupling functions are restricted to be scaled versions of a single function $\bar{f}(s) = \tan(s/2)$. If additionally, the phase biases $\{\phi_i\}_{\mathcal{N}}$ are fixed and are given as

$$\begin{aligned}\phi_1 &= \pi - 3/100, & \phi_2 &= \pi - 3/100, & \phi_3 &= 0, \\ \phi_4 &= -\pi + 1/100, & \phi_5 &= 0, & \phi_6 &= -\pi + 1/100, \\ \phi_7 &= -\pi/2, & \phi_8 &= 0, & \phi_9 &= 0,\end{aligned}\quad (9)$$

then we should first choose $\alpha_{ij} \in \mathbb{N}$ for each $(j, i) \in \mathcal{E}'$, so that

$$\operatorname{sgn}(\bar{f}(\alpha_{ij}\tilde{\Delta}_{ij} + \phi_i)) = \operatorname{sgn}(\bar{\omega} - \omega_i), \quad i \in \mathcal{N}.$$

This can be simply done as $\alpha_{12} = 1$, $\alpha_{21} = 2$, and $\alpha_{ij} = 1$ for all other edges. Finally, we choose $g_i > 0$ for each $i \in \mathcal{N}$ so that

$$g_i \bar{f}(\alpha_{ij}\tilde{\Delta}_{ij} + \phi_i) = \bar{\omega} - \omega_i.$$

The corresponding simulation result with different initial conditions is given in Figure 3. Note that we obtain the number of different shapes as 3. This is because only $(n_1, n_2) = (-1, 2), (0, 0), (0, 1), (0, 2), (1, -2), (1, -1), (1, 0)$ are possible, and they result in three different equivalence classes $\{(-1, 2)\} = \{(0, 0)\} = \{(1, -2)\}$, $\{(0, 1)\} = \{(1, -1)\}$, and $\{(0, 2)\} = \{(1, 0)\}$ (their differences are integer spans of the column of the Laplacian matrix, $(-1, 2)$). This is smaller than the number of different shapes for the network obtained in Example 1, because the smallest possible α_{78} is 1 and α_{87} is 4, and the number of different shapes even with $\alpha_{ij} = 1$ for all other edges (which makes the inverse of $\mathcal{L}|_{\mathcal{N} \setminus \{7,8\}}$ again the integer matrix) is 5.

On the other hand, if we allow freedom of choice with respect to the phase biases $\{\phi_i\}_{\mathcal{N}}$ in the above situation, then we can also take α_{21} as unity, by taking $\phi_1 = 1/25$

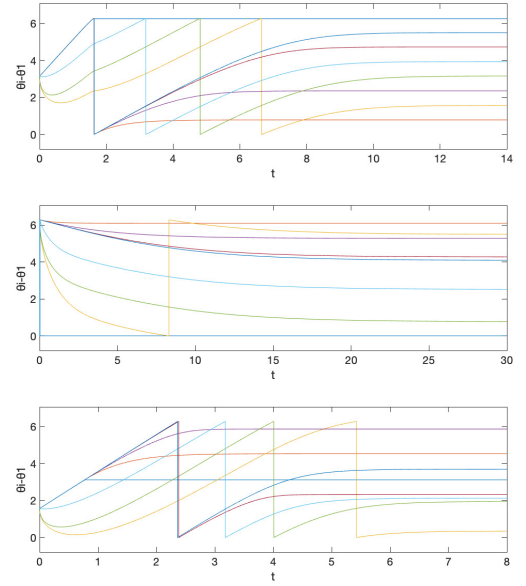


Figure 3: Simulation results for initial conditions (1) $\theta_1(0) = \pi$ (2) $\theta_1(0) = 0$ (3) $\theta_1(0) = -\pi/2$, where $\theta_i(0) = 0$, $i \neq 1$ for all cases. These correspond to the equivalence classes (1) $\{0, 1\}$ (2) $\{0, 0\}$ (3) $\{1, 0\}$. The equivalence class $\{0, 1\}$ corresponds to the objective formation. The graph represents the phase differences $\theta_i(t) - \theta_1(t)$, $i \neq 1$.

and $\phi_2 = -1/25$, and this gives almost global convergence. The simulation result with the initial condition that resulted in different shapes in Figure 3 is given in Figure 4(a). We observe that now we have convergence to the unique shape that was assigned. One can check that the number of different shapes is 1 in this case. In particular, only $(n_1, n_2) = (-1, 1), (0, 0), (1, -1)$ are possible, but they are all in the same equivalence class (their differences are integer spans of the column of the Laplacian matrix, $(-1, 1)$).

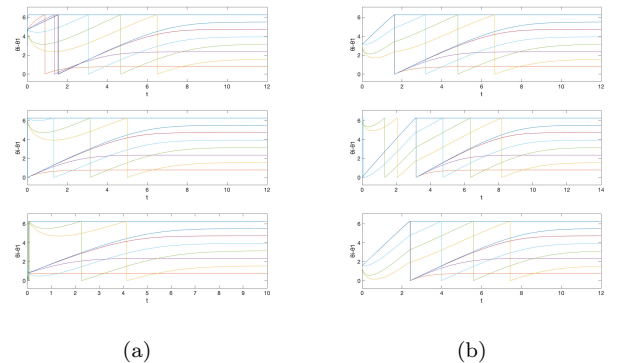


Figure 4: Simulation results for initial conditions (1) $\theta_1(0) = \pi$ (2) $\theta_1(0) = 0$ (3) $\theta_1(0) = -\pi/2$, where $\theta_i(0) = 0$, $i \neq 1$ for all cases, when (a) we allow the freedom of choice on the phase biases and (b) we saturate the prototypical barrier function. The graph represents the phase differences $\theta_i(t) - \theta_1(t)$, $i \neq 1$.

On the contrary, if we preserve the restriction that the phase biases $\{\phi_i\}_{\mathcal{N}}$ are fixed as (9), but, as in Remark 6, instead saturate the prototypical barrier function so that now $\bar{f}(s) : (-\pi, \pi) \rightarrow (-200 - \delta, 40 + \delta)$ with sufficiently small $\delta > 0$, then we again obtain almost global convergence. The saturation region is chosen so that $\bar{f}(\alpha_{ij}\tilde{\Delta}_{ij} + \phi_i) \in [-200, 40]$ for all $i \in \mathcal{N}$. Note that,

in this case, we must have $g_1 = 1/\tan(\pi/2 - 1/40)$ and $g_2 = 1/\tan(\pi/2 - 1/200)$. This is illustrated in Figure 4(b) with the same initial condition that resulted in a different shape in Figure 3. This happens because, for the preserved shapes, $\bar{\omega}$ should satisfy $\bar{\omega} - \omega_i \in (-g_i(200+\delta), g_i(40+\delta))$, $i \in \mathcal{N}$, hence from g_1 and g_2 , we get $\bar{\omega} \in (1 - \eta_1, 1 + \eta_2)$ with some small $\eta_1, \eta_2 > 0$. Since with the original coupling functions, different shapes had their common frequency bigger than 2 for $\{0, 0\}$ and smaller than 0 for $\{1, 0\}$, the trajectory must converge to the discontinuity boundary.

5.5. Simultaneous design of multiple shapes

We want to note that given a digraph $\mathcal{G} = (\mathcal{N}, \mathcal{E})$, a set of intrinsic frequencies $\{\omega_i\}_{\mathcal{N}}$, and a set of interconnection weights $\{\alpha_{ij}\}_{\mathcal{E}}$, it might be possible to assign multiple shapes $(\bar{\omega}^k, \{\Delta_{ij}^k\}_{\mathcal{E}})$, $k = 1, \dots, M$ when we have freedom of choice with respect to the set of phase biases $\{\phi_i\}_{\mathcal{N}}$ and the set of coupling functions $\{f_i(\cdot)\}_{\mathcal{N}}$. Of course, M should be smaller than or equal to the number of different shapes governed by $\{\alpha_{ij}\}_{\mathcal{E}}$.

In particular, from the monotonicity of the coupling function, a necessary and sufficient condition for the viability is

- the existence of $\phi_i \in (-\pi, \pi)$ such that $\Theta_i^k \in (-\pi, \pi)$ defined by $\Theta_i^k = \sum_{j \in \mathcal{N}_i} \alpha_{ij} \Delta_{ij}^k + \phi_i \bmod 2\pi$ has the same order as $\bar{\omega}^k$; if k_s is the sorted index such that

$$\bar{\omega}^{1_s} \leq \bar{\omega}^{2_s} \leq \dots \leq \bar{\omega}^{M_s},$$

then we should have, with equality being preserved:

$$\Theta_i^{1_s} \leq \Theta_i^{2_s} \leq \dots \leq \Theta_i^{M_s}, \quad i \in \mathcal{N}.$$

This is equivalent to $\bar{\omega}^k$ having the same order as $\Theta_i^k \bmod 2\pi$ for any ϕ_i . Hence, it is always possible when $M = 2$.

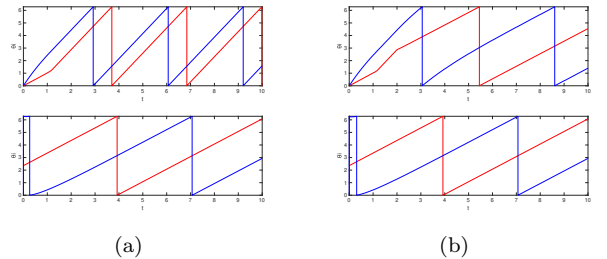
On the other hand, given a digraph $\mathcal{G} = (\mathcal{N}, \mathcal{E})$, a set of intrinsic frequencies $\{\omega_i\}_{\mathcal{N}}$, and multiple desired shapes $(\bar{\omega}^k, \{\Delta_{ij}^k\}_{\mathcal{E}})$, $k = 1, \dots, M$, it might be possible to select a set of interconnection weights $\{\alpha_{ij}\}_{\mathcal{E}}$ so that the above necessary and sufficient condition is fulfilled. However, in such cases, due to the choice of interconnection weights, in general, the number of different shapes increases.

Example 2. For graph $\mathcal{G} = (\{1, 2\}, \{(1, 2), (2, 1)\})$, if $\alpha_{12} = 1$ and $\alpha_{21} = 1$, $\phi_1 = \pi/2$ and $\phi_2 = \pi/2$, then we have two different shapes. If $\omega_1 = 0$, $\omega_2 = 2$, $\bar{\omega} = 1$, and $\Delta_{12} = \pi$, then we can set the other shape to be near the boundary, for instance, as $\bar{\omega}' = 2$ and $\Delta'_{12} = \pi/2 - \epsilon$, since $\Theta_1 = -\pi/2$, $\Theta'_1 = \pi - \epsilon$ and $\Theta_2 = -\pi/2$, $\Theta'_2 = \epsilon$. A suitable set of coupling functions is

$$f_1(s) = \frac{\tan\left(\frac{s}{2}\right) + \tan\left(\frac{\pi}{4}\right)}{\tan\left(\frac{\pi-\epsilon}{2}\right) + \tan\left(\frac{\pi}{4}\right)} + 1,$$

$$f_2(s) = \frac{\tan\left(\frac{s}{2}\right) + \tan\left(\frac{\pi}{4}\right)}{\tan\left(\frac{\epsilon}{2}\right) + \tan\left(\frac{\pi}{4}\right)} - 1.$$

Then, since only the other shape is near the boundary, with a persistent small kick on θ_1 or θ_2 , we have almost global convergence to the desired shape $\bar{\omega} = 1$ and $\Delta_{12} = \pi$. This is illustrated in Figure 5.



(a)

(b)

Figure 5: Simulation results for initial conditions (1) $\theta_1(0) = 0$, $\theta_2(0) = 0$ and (2) $\theta_1(0) = 3\pi/4$, $\theta_2(0) = 0$, when (a) there are no ‘kicks’ and (b) when there is a small persistent excitation given to θ_2 , which ‘kicks’ the trajectory from the near-boundary shape (1) to the robust shape (2). These correspond to the equivalence classes (1) $\{[0, 0]\}$ and (2) $\{[0, 1]\}$.

Example 3. Another example is given for the three agents that constitute a directed ring; $\mathcal{E} = \{(2, 1), (3, 2), (1, 3)\}$. From Remark 3, we notice that if $\phi_S = -\pi$, then the number of different n_S is two, and by the structure of the Laplacian matrix, if $\alpha_{ij} = 1$, for all $(j, i) \in \mathcal{E}$, then all the sequences associated with each n_S are equivalent (Section 4.3). Therefore, the number of different shapes becomes two. We assign for this network a uniformly distributed shape with two different permutations by letting

$$\bar{\omega}^1 = -1, \quad \Delta_1^1 = 0, \quad \Delta_2^1 = \frac{2\pi}{3}, \quad \Delta_3^1 = \frac{4\pi}{3},$$

$$\bar{\omega}^2 = 1, \quad \Delta_1^2 = 0, \quad \Delta_2^2 = \frac{4\pi}{3}, \quad \Delta_3^2 = \frac{2\pi}{3}.$$

To satisfy the above necessary and sufficient condition and to satisfy $\phi_S = \sum_{i=1}^3 \phi_i = -\pi$, we utilized

$$\phi_1 = -\frac{3\pi}{4}, \quad \phi_2 = -\frac{3\pi}{4}, \quad \phi_3 = \frac{\pi}{2}.$$

Then, for any intrinsic frequency ω_i , we can assign both shapes simultaneously. Here, we take $\omega_1 = -2$, $\omega_2 = 0$, and $\omega_3 = 2$. A suitable set of coupling functions is

$$f_1(s) = 2 \frac{\tan\left(\frac{s}{2}\right) + \tan\left(\frac{\pi}{24}\right)}{\tan\left(\frac{7\pi}{24}\right) + \tan\left(\frac{\pi}{24}\right)} + 1,$$

$$f_2(s) = 2 \frac{\tan\left(\frac{s}{2}\right) + \tan\left(\frac{\pi}{24}\right)}{\tan\left(\frac{7\pi}{24}\right) + \tan\left(\frac{\pi}{24}\right)} - 1,$$

$$f_3(s) = 2 \frac{\tan\left(\frac{s}{2}\right) + \tan\left(\frac{\pi}{12}\right)}{\tan\left(\frac{5\pi}{12}\right) - \tan\left(\frac{\pi}{12}\right)} - 1.$$

This is illustrated in Figure 6.

Example 4. The final example handles arbitrary odd number $N > 1$ with star shaped graph $\mathcal{G} = (\{1, \dots, N\}, \{(1, 2), \dots, (1, N), (2, 1)\})$. If $\alpha_{ij} = 1$ for all $(j, i) \in \mathcal{E}$, $\phi_1 = (N-1)\pi/N$ and $\phi_2 = 0$, then we have two different shapes. In particular, if $\omega_i = 0$ for all $i \in \mathcal{N}$, $\phi_i = 0$, $i = 2, \dots, (N+1)/2$ and $\phi_i = (N-1)\pi/N$, $i = (N+3)/2, \dots, N$, then we can assign two shapes, where one represents perfect balanced formation, i.e., $\bar{\omega} = 0$, $\Delta_i = 2(i-1)\pi/N$ for all $i = 1, \dots, N$, and the other represents perfect synchronization, i.e., $\bar{\omega}' = 1$, $\Delta'_i = 0$ for all $i = 1, \dots, N$. This is because, $0 = \bar{\omega} < \bar{\omega}' = 1$ and $-(N-1)\pi/N = \Theta_1 < \Theta'_1 = (N-1)\pi/N$,

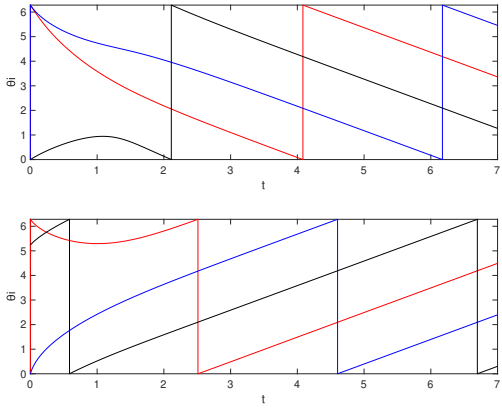


Figure 6: Simulation results for initial conditions (1) $\theta_i(0) = 0, i \in \mathcal{N}$ and (2) $\theta_1(0) = 0, \theta_2(0) = 0, \theta_3(0) = -\pi/3$. These correspond to the equivalence classes (1) $\{0, 0, 0\}$ and (2) $\{0, -1, 0\}$.

$-2(i-1)\pi/N = \Theta_i < \Theta'_i = 0, i = 2, \dots, (N+1)/2$, and $-(2i-N-1)\pi/N = \Theta_i < \Theta'_i = (N-1)\pi/N, i = (N+3)/2, \dots, N$. We can utilize coupling functions in the form of $f_i(s) = a_i \tan(s/2) + b_i$, where a_1 and b_1 form the unique solution of the linear equation

$$\begin{bmatrix} \tan(-\frac{N-1}{2N}\pi) & 1 \\ \tan(\frac{N-1}{2N}\pi) & 1 \end{bmatrix} \begin{bmatrix} a_1 \\ b_1 \end{bmatrix} = \begin{bmatrix} 0 \\ 1 \end{bmatrix}.$$

For $i = 2, \dots, (N+1)/2$, a_i and b_i form the unique solution of the linear equation

$$\begin{bmatrix} \tan(-\frac{i-1}{N}\pi) & 1 \\ \tan(0) & 1 \end{bmatrix} \begin{bmatrix} a_i \\ b_i \end{bmatrix} = \begin{bmatrix} 0 \\ 1 \end{bmatrix}.$$

For $i = (N+3)/2, \dots, N$, a_i and b_i form the unique solution of the linear equation

$$\begin{bmatrix} \tan(-\frac{2i-N-1}{2N}\pi) & 1 \\ \tan(\frac{N-1}{2N}\pi) & 1 \end{bmatrix} \begin{bmatrix} a_i \\ b_i \end{bmatrix} = \begin{bmatrix} 0 \\ 1 \end{bmatrix}.$$

This is illustrated in Figure 7 for the case when $N = 9$.

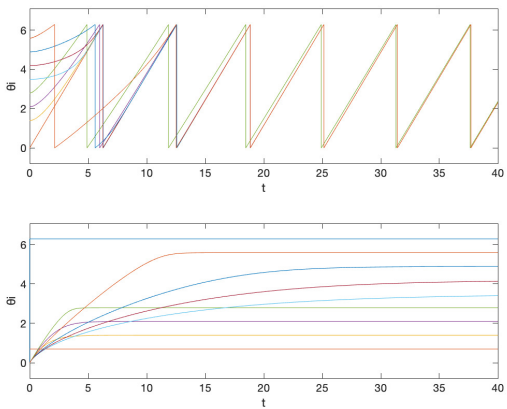


Figure 7: Simulation results for initial conditions (1) $\theta_2(0) = 0$ and $\theta_i(0) = 2(i-1)\pi/N, i \neq 2$ and (2) $\theta_2(0) = 2\pi/N$ and $\theta_i(0) = 0, i \neq 2$.

6. Conclusion

By introducing the node-wise monotone barrier coupling law, we proposed a tool to simultaneously assign

multiple central patterns on the circle, where a transition between different patterns can happen via a simple kick. This shows one of the benefits of using a nonlinear coupling, especially in the emergence of collective behaviors, and is motivated by CPGs. We characterized the shape of the generated central patterns, identified the number of different shapes, analyzed the viability of assigning desired patterns, and provided design guidelines.

Compared with our initial work [24], where instead of the node-wise monotone barrier coupling law, we have utilized the edge-wise version

$$\dot{\theta}_i = \omega_i + \sum_{j \in \mathcal{N}_i} f_{ij}(\theta_j - \theta_i),$$

now we do not have to confine ourselves to undirected graphs $\mathcal{G} = (\mathcal{N}, \mathcal{E})$. The analysis of the generated shape has become less straightforward, but instead, we obtained a general understanding of the number of different shapes. From a design perspective, for a similar number of restrictions, we now have fewer limitations and more straightforward design guidelines.

Future consideration will be given to extension of the framework to other nonlinear spaces and its use in practical design problems. An example is to control a cluster of drones. For instance, in a situation where a fleet of drones move in a balanced formation until they encounter obstacles, e.g., a scenario in which they have to pass between two buildings, and this impulsive event is detected by some of the drones in the formation. Then, this ‘kick’ could alternate the formation of the network, for example, to a line, so that they can be safely guided through a narrow passage.

Acknowledgement

The authors are most grateful to Professor Rodolphe Sepulchre for inspiring this work and for his guidance and support.

References

- [1] M. Maghenem, E. Panteley, A. Loría, Singular-perturbations-based analysis of synchronization in heterogeneous networks: A case-study, in: Proceedings of the 55th IEEE Conference on Decision and Control, 2016, pp. 2581–2586.
- [2] J. G. Lee, H. Shim, Heterogeneous Van der Pol oscillators under strong coupling, in: Proceedings of the 57th IEEE Conference on Decision and Control, 2018, pp. 3666–3673.
- [3] L. Tumash, E. Panteley, A. Zakharova, E. Schöll, Synchronization patterns in Stuart–Landau networks: a reduced system approach, The European Physical Journal B 92 (2019) 100.
- [4] J. G. Lee, H. Shim, Behavior of a network of heterogeneous Liénard systems under strong output coupling, IFAC-PapersOnLine 52 (16) (2019) 256–261.
- [5] E. Panteley, A. Loría, Synchronization and dynamic consensus of heterogeneous networked systems, IEEE Transactions on Automatic Control 62 (8) (2017) 3758–3773.
- [6] J. G. Lee, H. Shim, A tool for analysis and synthesis of heterogeneous multi-agent systems under rank-deficient coupling, Automatica 117 (2020) 108952.
- [7] H. Yun, H. Shim, H.-S. Ahn, Initialization-free privacy-guaranteed distributed algorithm for economic dispatch problem, Automatica 102 (2019) 86–93.
- [8] J. G. Lee, H. Shim, A distributed algorithm that finds almost best possible estimate under non-vanishing and time-varying measurement noise, IEEE Control Systems Letters 4 (1) (2020) 229–234.

[9] J. G. Lee, J. Kim, H. Shim, Fully distributed resilient state estimation based on distributed median solver, *IEEE Transactions on Automatic Control* 65 (9) (2020) 3935–3942.

[10] M. Guo, B. Jayawardhana, J. G. Lee, H. Shim, Simultaneous distributed localization, mapping and formation control of mobile robots based on local relative measurements, *IFAC-PapersOnLine* 53 (2) (2020) 9614–9620.

[11] R. Sepulchre, D. Paley, N. E. Leonard, Collective motion and oscillator synchronization, in: V. Kumar, N. E. Leonard, and A. S. Morse (Eds.), *Cooperative Control*. Lecture Notes in Control and Information Science. Springer, Berlin, Heidelberg, 2005, pp. 189–205.

[12] L. Scardovi, A. Sarlette, R. Sepulchre, Synchronization and balancing on the N-torus, *Systems & Control Letters* 56 (5) (2007) 335–341.

[13] A. Sarlette, S. Bonnabel, R. Sepulchre, Coordinated motion design on Lie groups, *IEEE Transactions on Automatic Control* 55 (5) (2010) 1047–1058.

[14] C. Mostajeran, R. Sepulchre, Positivity, monotonicity, and consensus on Lie groups, *SIAM Journal on Control and Optimization* 56 (3) (2018) 2436–2461.

[15] J. Markdahl, J. Thunberg, J. Gonçalves, Almost global consensus on the n -sphere, *IEEE Transactions on Automatic Control* 63 (6) (2018) 1664–1675.

[16] A. Sarlette, R. Sepulchre, Consensus optimization on manifolds, *SIAM Journal on Control and Optimization* 48 (1) (2009) 56–76.

[17] J. Markdahl, J. Thunberg, J. Gonçalves, High-dimensional Kuramoto models on Stiefel manifolds synchronize complex networks almost globally, *Automatica* 113 (2020) 108736.

[18] G. Drion, A. Franci, R. Sepulchre, Cellular switches orchestrate rhythmic circuits, *Biological Cybernetics* 113 (2019) 71–82.

[19] J. G. Lee, R. Sepulchre, Rapid synchronization under weak synaptic coupling, in: *Proceedings of the 59th IEEE Conference on Decision and Control*, 2020, pp. 6168–6173.

[20] J. G. Lee, R. Sepulchre, Rapid and robust synchronization via weak synaptic coupling, under preparation for *IEEE Transactions on Automatic Control*.

[21] A. J. Ijspeert, Central pattern generators for locomotion control in animals and robots: A review, *Neural Networks* 21 (4) (2008) 642–653.

[22] D. Somers, N. Kopell, Rapid synchronization through fast threshold modulation, *Biological Cybernetics* 68 (1993) 393–407.

[23] D. Angeli, S. Manfredi, A Petri Net approach to consensus in networks with joint-agent interactions, *Automatica* 110 (2019) 108466.

[24] C. Mostajeran, J. G. Lee, G. Van Goffrier, R. Sepulchre, Target formation on the circle by monotone system design, in: *Proceedings of the 60th IEEE Conference on Decision and Control*, 2021, pp. 7099–7104.

[25] R. Sepulchre, Consensus on nonlinear spaces, *Annual Reviews in Control* 35 (1) (2011) 56–64.

[26] L. Farina, S. Rinaldi, *Positive linear systems: Theory and applications*, Wiley, 2000.

[27] P. De Leenheer, D. Aeyels, Stabilization of positive linear systems, *Systems & Control Letters* 44 (4) (2001) 259–271.

[28] H. M. Hårdin, J. H. van Schuppen, Observers for linear positive systems, *Linear Algebra and its Applications* 425 (2-3) (2007) 571–607.

[29] A. Rantzer, Distributed control of positive systems, in: *Proceedings of the 50th IEEE Conference on Decision and Control*, 2011, pp. 6608–6611.

[30] D. Angeli, J. E. Ferrell, E. D. Sontag, Detection of multistability, bifurcations, and hysteresis in a large class of biological positive-feedback systems, *Proceedings of the National Academy of Sciences of the United States of America* 101 (7) (2004) 1822–1827.

[31] F. Forni, R. Sepulchre, Differentially positive systems, *IEEE Transactions on Automatic Control* 61 (2) (2016) 346–359.

[32] C. Mostajeran, R. Sepulchre, Monotonicity on homogeneous spaces, *Mathematics of Control, Signals, and Systems* 30 (2018) 22.

[33] F. Forni, R. Sepulchre, Differential dissipativity theory for dominance analysis, *IEEE Transactions on Automatic Control* 64 (6) (2019) 2340–2351.

[34] V. D. Blondel, J. M. Hendrickx, A. Olshevsky, J. N. Tsitsiklis, Convergence in multiagent coordination, consensus, and flocking, in: *Proceedings of the 44th IEEE Conference on Decision and Control*, 2005, pp. 2996–3000.

[35] A. Olshevsky, J. N. Tsitsiklis, On the nonexistence of quadratic Lyapunov functions for consensus algorithms, *IEEE Transactions on Automatic Control* 53 (11) (2008) 2642–2645.

[36] F. Forni, Differential positivity on compact sets, in: *Proceedings of the 54th IEEE Conference on Decision and Control*, 2015, pp. 6355–6360.

[37] L. Moreau, Stability of continuous-time distributed consensus algorithms, in: *Proceedings of the 43rd IEEE Conference on Decision and Control*, 2004, pp. 3998–4003.

[38] L. Moreau, Stability of multiagent systems with time-dependent communication links, *IEEE Transactions on Automatic Control* 50 (2) (2005) 169–182.

[39] R. Olfati-Saber, J. A. Fax, R. M. Murray, Consensus and cooperation in networked multi-agent systems, *Proceedings of the IEEE* 95 (1) (2007) 215–233.

[40] A. Jadbabaie, J. Lin, A. S. Morse, Coordination of groups of mobile autonomous agents using nearest neighbor rules, *IEEE Transactions on Automatic Control* 48 (6) (2003) 988–1001.

[41] R. Sepulchre, D. A. Paley, N. E. Leonard, Stabilization of planar collective motion: All-to-all communication, *IEEE Transactions on Automatic Control* 52 (5) (2007) 811–824.

[42] R. Sepulchre, D. A. Paley, N. E. Leonard, Stabilization of planar collective motion with limited communication, *IEEE Transactions on Automatic Control* 53 (3) (2008) 706–719.

[43] A. Sarlette, R. Sepulchre, Synchronization on the circle, in: J. Dubbeldam, K. Green, and D. Lenstra (Eds.), *The complexity of dynamical systems*. Wiley, available at [arXiv:0901.2408](https://arxiv.org/abs/0901.2408), 2011.

[44] A. Sarlette, S. E. Tuna, V. D. Blondel, R. Sepulchre, Global synchronization on the circle, *IFAC Proceedings Volumes* 41 (2) (2008) 9045–9050.

[45] R. Bertollo, E. Panteley, R. Postoyan, L. Zaccarian, Uniform global asymptotic synchronization of Kuramoto oscillators via hybrid coupling, *IFAC-PapersOnLine* 53 (2) (2020) 5819–5824.

Appendix A. Graph theoretical preliminaries

In this subsection, we briefly summarize the graph theoretical concepts which are crucial for the investigation of multi-agent system (3) and their underlying network topology. We also provide an essential lemma associated with the structure of a given graph.

A (weighted directed) graph is a pair $\mathcal{G} = (\mathcal{N}, \mathcal{E})$ consisting of a finite nonempty set of nodes $\mathcal{N} = \{1, 2, \dots, N\}$ and an edge set of ordered pairs of nodes $\mathcal{E} \subseteq \mathcal{N} \times \mathcal{N}$, where $(i, i) \notin \mathcal{E}$ for all $i \in \mathcal{N}$ (i.e., the graph does not contain self-loops). The set $\mathcal{N}_i = \{j \in \mathcal{N} \mid (j, i) \in \mathcal{E}\}$ denotes the neighbors of the node i . A tuple $(i_0, i_1, \dots, i_l) \in \mathcal{N}^{l+1}$ is called a *path* (of length l) from the node i_0 to the node i_l , if $i_k \in \mathcal{N}_{i_{k+1}}$ for all $k = 0, \dots, l-1$. If i_1, \dots, i_l are distinct, then the path is called *elementary*. A *loop* is an elementary path with $i_0 = i_l$.

\mathcal{G} is called *undirected*, if $(j, i) \in \mathcal{E}$ implies $(i, j) \in \mathcal{E}$. Given a graph $\mathcal{G} = (\mathcal{N}, \mathcal{E})$, let $\mathcal{N}' \subseteq \mathcal{N}$ and

$$\mathcal{E}' \subseteq \mathcal{E}|_{\mathcal{N}'} := \{(j, i) \in \mathcal{E} \mid i, j \in \mathcal{N}'\}.$$

Then the pair $\mathcal{G}' = (\mathcal{N}', \mathcal{E}')$ is called a *subgraph* of \mathcal{G} . If $\mathcal{N}' = \mathcal{N}$, then \mathcal{G}' is a spanning subgraph. If a graph \mathcal{G} is *connected*, then there exists an agent i , from which information can propagate to all other agents j along paths in \mathcal{G} . A spanning subgraph \mathcal{T} of \mathcal{G} obtained by removing all edges that do not belong to one of these paths is called a *spanning tree* of \mathcal{G} .

We like to stress that for any connected digraph \mathcal{G} , the indices can be well assigned so that the Laplacian matrix associated with the graph can be written as

$$\mathcal{L} = \begin{bmatrix} \mathcal{L}_s & 0 \\ -\mathcal{A}_{sf} & \mathcal{L}_f + \mathcal{D}_f \end{bmatrix} \in \mathbb{R}^{N \times N},$$

where $\mathcal{L}_s \in \mathbb{R}^{|\mathcal{S}| \times |\mathcal{S}|}$ and $\mathcal{L}_f \in \mathbb{R}^{(N-|\mathcal{S}|) \times (N-|\mathcal{S}|)}$ are the Laplacian matrices of the unique iSCC, \mathcal{S} , and the subgraph induced by the rest of the agents, respectively. Since \mathcal{L}_s is the Laplacian matrix of a strongly connected graph, it is known that there exists a vector $\zeta := \text{col}(\zeta_1, \dots, \zeta_{|\mathcal{S}|}) \in \mathbb{R}^{|\mathcal{S}|}$ which satisfies $\zeta^T \mathcal{L}_s = 0$ and $\zeta_i > 0$ for all $i = 1, \dots, |\mathcal{S}|$. In particular, we have $\text{col}(\zeta, 0)^T \mathcal{L} = 0$.

The following lemma is essential in the proof of Theorem 2, which is given in Appendix B.

Lemma 1. *Under Assumption 1, for any $\mathcal{I} \subsetneq \mathcal{N}$ such that $\mathcal{S} \setminus \mathcal{I} \neq \emptyset$, where \mathcal{S} denotes the unique iSCC, there exists $\zeta_i > 0$, $i \in \mathcal{I}$ such that for any vector $\chi = [\chi_i] \in \mathbb{R}^N$,*

$$\sum_{i \in \mathcal{I}} \zeta_i \sum_{j \in \mathcal{N}} \alpha_{ij} (\chi_j - \chi_i) = \sum_{j \in \mathcal{N} \setminus \mathcal{I}} \beta_j \chi_j - \sum_{i \in \mathcal{I}} \gamma_i \chi_i \quad (\text{A.1})$$

with some coefficients $\beta_j, \gamma_i \geq 0$. Moreover, there exists $j^* \in \mathcal{N} \setminus \mathcal{I}$ and $i^* \in \mathcal{I}$ such that $\beta_{j^*} > 0$ and $\gamma_{i^*} > 0$.

PROOF. Consider a subgraph $\mathcal{G}_{\mathcal{I}} = (\mathcal{I}, \mathcal{E}|_{\mathcal{I}})$. Then, there exists iSCCs denoted as $\mathcal{S}^p \subset \mathcal{I}$, $p \in \mathcal{M} := \{1, \dots, M\}$, and the rest, denoted as $\mathcal{R} \subset \mathcal{I}$. We will first assume that Lemma 1 holds for the index set \mathcal{R} ; that is $\zeta_i > 0$ is given for $i \in \mathcal{R}$ such that for any vector $\chi = [\chi_i] \in \mathbb{R}^N$,

$$\begin{aligned} \sum_{i \in \mathcal{R}} \zeta_i \sum_{j \in \mathcal{N}} \alpha_{ij} (\chi_j - \chi_i) \\ = \sum_{j \in \mathcal{N} \setminus \mathcal{I}} \bar{\beta}_j \chi_j + \sum_{p=1}^M \sum_{j \in \mathcal{S}^p} \bar{\beta}_j \chi_j - \sum_{i \in \mathcal{R}} \gamma_i \chi_i, \end{aligned}$$

then we will show that for each $p \in \mathcal{M}$, we can find $\zeta_i > 0$, $i \in \mathcal{S}^p$ such that for any vector $\chi = [\chi_i] \in \mathbb{R}^N$,

$$\begin{aligned} \sum_{i \in \mathcal{S}^p} \zeta_i \sum_{j \in \mathcal{N}} \alpha_{ij} (\chi_j - \chi_i) = \sum_{j \in \mathcal{N} \setminus \mathcal{I}} \beta_j \chi_j - \sum_{i \in \mathcal{S}^p} \bar{\gamma}_i \chi_i \quad \text{and} \\ \bar{\gamma}_i > \bar{\beta}_i, \quad \forall i \in \mathcal{S}^p. \end{aligned} \quad (\text{A.2})$$

This will complete the proof. By repeating this argument (i.e., by replacing the role of \mathcal{I} with \mathcal{R}), we arrive after finitely many steps at the stage of assuming that Lemma 1 holds for the index set \mathcal{R} , but \mathcal{R} is empty; that is the subgraph $\mathcal{G}_{\mathcal{I}}$ only consists of iSCCs, so that the assumption holds trivially.

Let us carry out the above described proof steps. For this purpose, note that by Assumption 1 and the fact that $\mathcal{S} \setminus \mathcal{I} \neq \emptyset$, for each $p \in \mathcal{M}$, there always is $j \in \mathcal{N} \setminus \mathcal{I}$ and $i \in \mathcal{S}^p$ such that $(j, i) \in \mathcal{E}$.⁷ Now, let \mathcal{L}^p denote the Laplacian matrix of the subgraph $\mathcal{G}^p = (\mathcal{S}^p, \mathcal{E}|_{\mathcal{S}^p})$. Then, (A.2) for only those corresponding to \mathcal{S}^p can be represented as

$$(\zeta^p)^T (\mathcal{L}^p + \mathcal{D}^p) = (\bar{\gamma}^p)^T > (\bar{\beta}^p)^T$$

with some diagonal matrix $\mathcal{D}^p \geq 0$ such that $\mathcal{D}^p \neq 0$ by the existence of $(j, i) \in \mathcal{E}$, $j \in \mathcal{N} \setminus \mathcal{I}$, $i \in \mathcal{S}^p$. So, first let ξ_1^p be the left eigenvector of \mathcal{L}^p associated with the zero eigenvalue. Then, we have $\xi_1^p > 0$ and

$$(\xi_1^p)^T (\mathcal{L}^p + \mathcal{D}^p) = (\xi_1^p)^T \mathcal{D}^p \geq 0.$$

⁷This is because, otherwise \mathcal{S}^p becomes the unique iSCC \mathcal{S} of the entire graph, but this is not possible, since $\mathcal{S} \setminus \mathcal{I} \neq \emptyset$.

Now, let $\mathcal{N}'_1 \subset \mathcal{S}^p$ be the set of all indices $i \in \mathcal{S}^p$ such that the element of $(\xi_1^p)^T \mathcal{D}^p$ corresponding to agent i is positive. Clearly, \mathcal{N}'_1 is not empty. Now, we can always find sufficiently small $\varepsilon_1 > 0$ such that⁸

$$\xi_2^p := \xi_1^p - \varepsilon_1 1_{\mathcal{N}'_1} > 0$$

satisfies

$$(\xi_2^p)^T (\mathcal{L}^p + \mathcal{D}^p) = -\varepsilon_1 1_{\mathcal{N}'_1}^T (\mathcal{L}^p + \mathcal{D}^p) + (\xi_1^p)^T \mathcal{D}^p \geq 0$$

and that $\mathcal{N}'_1 \subsetneq \mathcal{N}'_2$. In particular,

$$\mathcal{N}'_2 = \mathcal{N}'_1 \cup \bigcup_{i \in \mathcal{N}'_1} \{j \in \mathcal{S}^p \mid (j, i) \in \mathcal{E}\}.$$

Therefore, by repeating this argument, due to the fact that \mathcal{G}^p is strongly connected, we arrive after finitely many steps at the situation where $\mathcal{N}'_k = \mathcal{S}^p$. This implies that

$$(\xi_k^p)^T (\mathcal{L}^p + \mathcal{D}^p) > 0.$$

Therefore, we can find sufficiently large $K > 0$ such that $\zeta^p := K \xi_k^p > 0$ satisfies

$$(\zeta^p)^T (\mathcal{L}^p + \mathcal{D}^p) > (\bar{\beta}^p)^T$$

and we conclude (A.2) as desired.

Appendix B. Proof of Theorem 2

The proof is done by a contradiction. We first focus on the forward invariance. Suppose that there is a particular solution of (3) such that $\theta \in \mathbb{T}_{\pi}^N$ holds only for a finite time interval $[0, T)$ and is violated at $t = T$. This implies that there is a time sequence $\{\tau_k\}$ such that τ_k is strictly increasing and $\lim_{k \rightarrow \infty} \tau_k = T$, and

$$\mathcal{I}_+(\{\tau_k\}) := \left\{ i \in \mathcal{N} : \lim_{k \rightarrow \infty} \nu_i(\tau_k) + \phi_i = (2n_i + 1)\pi \right\}$$

is non-empty,

or

$$\mathcal{I}_-(\{\tau_k\}) := \left\{ i \in \mathcal{N} : \lim_{k \rightarrow \infty} \nu_i(\tau_k) + \phi_i = (2n_i - 1)\pi \right\}$$

is non-empty,

where $n_i \in \mathbb{N}$ is such that $\nu_i(0) + \phi_i \in ((2n_i - 1)\pi, (2n_i + 1)\pi)$.⁹ Let us first assume that $\mathcal{I}_+(\{\tau_k\})$ is non-empty. We will first show that a contradiction occurs if $\mathcal{S} \subset \mathcal{I}_+(\{\tau_k\})$, where \mathcal{S} denotes the unique iSCC. If $\mathcal{S} \setminus \mathcal{I}_+(\{\tau_k\}) \neq \emptyset$, we will then show that it is possible to construct another time sequence $\{\bar{\tau}_k\}$ (based on $\{\tau_k\}$), such that

$$|\mathcal{I}_+(\{\tau_k\})| < |\mathcal{I}_+(\{\bar{\tau}_k\})| \quad (\text{B.1})$$

where the notation $|\cdot|$ implies the cardinality of the set. By repeating this argument (i.e., by replacing the role of $\{\tau_k\}$ with $\{\bar{\tau}_k\}$), we arrive after finitely many steps at the index set $\mathcal{I}_+(\{\tau_k\})$ such that $\mathcal{S} \subset \mathcal{I}_+(\{\tau_k\})$, which yields a contradiction. This means that there is no such sequence

⁸ $1_{\mathcal{I}}$ is the vector of appropriate size with 1 only in the position that corresponds to the index set \mathcal{I} and 0 elsewhere.

⁹This implies $\nu_i(t) + \phi_i \in ((2n_i - 1)\pi, (2n_i + 1)\pi)$ for all $t \in [0, T)$.

$\{\tau_k\}$ that makes $\mathcal{I}_+(\{\tau_k\})$ non-empty. Similarly, it can be seen that there is no sequence that makes $\mathcal{I}_-(\{\tau_k\})$ non-empty. Therefore, we conclude there is no such finite time T , and thus $\theta(t) \in \mathbb{T}_\pi^N$ for all $t \geq 0$. Given the forward invariance in \mathbb{T}_π^N , the convergence to an integral curve can be shown similarly as in [14].

Let us carry out the steps of the proof described above. For convenience, we write \mathcal{I} instead of $\mathcal{I}_+(\{\tau_k\})$ in the following. Note that, by the definition of \mathcal{I} , for each $\eta > 0$, there exists a sufficiently large $k^* \in \mathbb{N}$ such that $\nu_i(\tau_k) + \phi_i > (2n_i + 1)\pi - \eta$ for all $k \geq k^*$. Hence, if $\mathcal{S} \subset \mathcal{I}$, then for any given set of positive coefficients ζ_i , $i \in \mathcal{S}$, there is k such that¹⁰

$$\sum_{i \in \mathcal{S}} \zeta_i \nu_i(t) = \sum_{j \in \mathcal{N}} \alpha_{ij} \cdot (\theta_j(\tau_k) - \theta_i(\tau_k)) \neq 0.$$

However, this is violated if ζ_i , $i \in \mathcal{S}$ corresponds to the elements of the left eigenvector of the Laplacian matrix associated with the zero eigenvalue, because then

$$\sum_{i \in \mathcal{S}} \zeta_i \sum_{j \in \mathcal{N}} \alpha_{ij} (\theta_j(t) - \theta_i(t)) \equiv 0, \quad \forall t \in [0, T].$$

Hence we have shown that $\mathcal{S} \subset \mathcal{I}$ is not possible and we continue the proof for the case that $\mathcal{S} \setminus \mathcal{I} \neq \emptyset$. For this purpose, let

$$W(t) := \sum_{i \in \mathcal{I}} \zeta_i \nu_i(t) = \sum_{i \in \mathcal{I}} \zeta_i \sum_{j \in \mathcal{N}} \alpha_{ij} \cdot (\theta_j(t) - \theta_i(t)),$$

where $\zeta_i > 0$, $i \in \mathcal{I}$ is given by Lemma 1 considering the index set $\mathcal{I} \subsetneq \mathcal{N}$. Note that $W(t)$ is continuously differentiable, $W(t) < \sum_{i \in \mathcal{I}} \zeta_i ((2n_i + 1)\pi - \phi_i) =: \bar{W}_\mathcal{I}$ on $[0, T]$, and $\lim_{k \rightarrow \infty} W(\tau_k) = \bar{W}_\mathcal{I}$. Let us now consider a strictly decreasing sequence $\{\varepsilon_q\}$ of positive numbers such that $\lim_{q \rightarrow \infty} \varepsilon_q = 0$ and that $W(0) < \bar{W}_\mathcal{I} - \varepsilon_0$. Choose a subsequence $\{\tau_{k_q}\}_{q \in \mathbb{N}}$ of $\{\tau_k\}$ such that

$$W(\tau_{k_q}) \geq \bar{W}_\mathcal{I} - \frac{\varepsilon_q}{2}, \quad \forall q \in \mathbb{N}. \quad (\text{B.2})$$

Based on this subsequence, we now construct a sequence $\{s_q\}_{q \in \mathbb{N}}$ such that (see Figure B.8)

$$s_q := \max \{s \in [0, \tau_{k_q}] \mid W(s) = \bar{W}_\mathcal{I} - \varepsilon_q\}. \quad (\text{B.3})$$

By (B.2) and (B.3), the sequence $\{s_q\}$ is strictly increasing and $\lim_{q \rightarrow \infty} s_q = T$. Moreover, since $\lim_{q \rightarrow \infty} W(s_q) = \bar{W}_\mathcal{I}$,

$$\lim_{q \rightarrow \infty} \nu_i(s_q) + \phi_i = (2n_i + 1)\pi, \quad \forall i \in \mathcal{I}. \quad (\text{B.4})$$

In addition, from (B.2) and (B.3), it follows that $s_q < \tau_{k_q}$ and

$$\dot{W}(s_q) \geq 0, \quad \forall q \in \mathbb{N}. \quad (\text{B.5})$$

On the other hand, if we compute \dot{W} , then we have

$$\begin{aligned} \dot{W}(t) &= \sum_{i \in \mathcal{I}} \zeta_i \sum_{j \in \mathcal{N}} \alpha_{ij} (\omega_j - \omega_i) \\ &\quad + \sum_{i \in \mathcal{I}} \zeta_i \sum_{j \in \mathcal{N}} \alpha_{ij} (f_j(t) - f_i(t)), \end{aligned}$$

¹⁰This is because, if $\sum_{i \in \mathcal{S}} \zeta_i ((2n_i + 1)\pi - \phi_i) = 0$, then the sum converges to zero but is negative for all finite k , and otherwise if $\sum_{i \in \mathcal{S}} \zeta_i ((2n_i + 1)\pi - \phi_i) \neq 0$, then there exists sufficiently small η such that the sum is non-zero for all $k \geq k^*$.

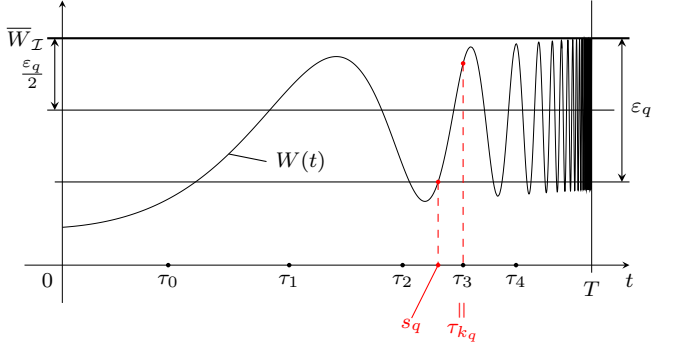


Figure B.8: Illustration of the choice of the sequence $\{s_q\}_{q \in \mathbb{N}}$ based on $\{\tau_k\}_{k \in \mathbb{N}}$.

where $f_k(t) := f_k(\nu_k(t) + \phi_k)$, $k \in \mathcal{N}$, for simplicity. We denote the first sum by M_0 . Invoking Lemma 1 for the index set \mathcal{I} , we therefore have that $(\beta_j, \gamma_i \geq 0)$

$$\dot{W}(t) \leq M_0 + \sum_{j \in \mathcal{N} \setminus \mathcal{I}} \beta_j f_j(t) - \sum_{i \in \mathcal{I}} \gamma_i f_i(t). \quad (\text{B.6})$$

Let $\mathcal{J} := \mathcal{N} \setminus \mathcal{I}$ (which is non-empty). Then, (B.5) and (B.6) yield

$$\sum_{j \in \mathcal{J}} \beta_j f_j(s_q) \geq \sum_{i \in \mathcal{I}} \gamma_i f_i(s_q) - M_0 =: M_q.$$

Again by Lemma 1, at least one β_j (γ_i), where $j \in \mathcal{J}$ ($i \in \mathcal{I}$), is positive. Thus, it follows from (B.4) that $M_q \rightarrow \infty$ as $q \rightarrow \infty$. Since

$$\sum_{j \in \mathcal{J}} \beta_j f_j(s_q) \leq \bar{\beta} \sum_{j \in \mathcal{J}} \max \{f_j(s_q), 0\}$$

where $\bar{\beta} := \max_{j \in \mathcal{J}} \beta_j > 0$, we have

$$\sum_{j \in \mathcal{J}} \max \{f_j(s_q), 0\} \geq \frac{M_q}{\bar{\beta}}. \quad (\text{B.7})$$

Therefore, for each sufficiently large q , there is an index $j_q \in \mathcal{J}$ such that $f_{j_q}(s_q) \geq M_q / (|\mathcal{J}| \bar{\beta})$. Since \mathcal{J} is a finite set, there is a subsequence $\{\bar{\tau}_k\} = \{s_{q_k}\}$ such that $j^* = j_{q_k} \in \mathcal{J}$; hence

$$f_{j^*}(\nu_{j^*}(\bar{\tau}_k) + \phi_{j^*}) \rightarrow \infty$$

i.e., $\nu_{j^*}(\bar{\tau}_k) + \phi_{j^*} \rightarrow (2n_{j^*} + 1)\pi$. Consequently,

$$\mathcal{I}_+(\{\tau_k\}) \stackrel{(\text{B.4})}{\subseteq} \mathcal{I}_+(\{s_q\}) \subseteq \mathcal{I}_+(\{\bar{\tau}_k\}).$$

By construction, $j^* \in \mathcal{I}_+(\{\bar{\tau}_k\}) \setminus \mathcal{I}_+(\{\tau_k\})$ and we can conclude (B.1) as desired.

Noting that the above proof holds even if we let $T = \infty$ —so that there is no time sequence $\{\tau_k\}$ such that τ_k is strictly increasing and $\lim_{k \rightarrow \infty} \tau_k = \infty$ which makes $\mathcal{I}_+(\{\tau_k\})$ ($\mathcal{I}_-(\{\tau_k\})$) non-empty—it follows that the control input $f_i(\nu_i(t) + \phi_i)$ is bounded uniformly on $[0, T) = [0, \infty)$.